

Enantioselective Synthesis of (-)-Tetrabenazine Via Continuous Crystallization-Induced Diastereomer Transformation

Supporting Information

Andrew J. Kukor,^a Noah Depner,^a Isabelle Cai,^a John L. Tucker,^b Jeffrey C. Culhane^b and Jason E. Hein^{*a}

^a Department of Chemistry, The University of British Columbia, Vancouver, BC V6T 1Z1, Canada

^b Neurocrine Biosciences, San Diego, California, 92130, United States

*email for J.E.H.: jhein@chem.ubc.ca

Table of Contents

1. General Info	6
a. Chemical Suppliers	6
b. Equipment Setup	6
c. Analytical Methods	7
2. System Hardware and Configurations	8
a. VapourTec Flow System	8
b. CIDT System – Configuration #1	9
c. CIDT System – Configuration #2	10
d. Inline Racemization Chamber	10
3. Webcam Turbidity Measurements	11
a. Software	11
b. Hardware	11
c. Automated Solubility Curve iControl Procedure	12
4. Synthetic Procedures	12
a. Tetrabenazine (TBZ)	12
b. Enantiopure (-)-TBZ·(-)-CSA (3)	13
c. (-)-TBZ·(-)-CSA (3), 70% e.e.	13
d. (-)-TBZ·(-)-CSA, ~0% e.e. (4)	13
5. Calibration and Standard Additions	13
a. Background	13
b. Procedure	13
c. Sample Raw Data – Solubility Curve Experiment	14
d. Sample Calibration Curves – Solubility Curve Experiment	15
6. Experimental Procedures	15
a. General Manual Sampling Procedure	15
b. General Automated Solubility Curve Procedure – Figure 3 and Figure SI 10-13	16
c. General VapourTec Racemization Procedure – Figure 4 and Figure 14-16	16
d. Solubility Curve Procedure – Figure 6 and Figure SI 8, 9, 17 and 18	16
e. CIDT: Solids Transfer Procedure – Figure 7, Figure SI 19	17

f. CIDT: Racemization Procedure – Figure 4, Figure SI 20	17
g. CIDT: Final Experiment Procedure – Figure 9 and Figure SI 21 and 22	18
7. Additional Experimental Data	20
a. (-)-TBZ•(-)-CSA Solubility in 100% Acetone	20
b. (-)-TBZ•(-)-CSA Solubility in 75% Acetone/25% Water	20
c. (-)-TBZ•(-)-CSA Solubility in 50% Acetone/50% Water	21
d. (-)-TBZ•(-)-CSA Solubility in 25% Acetone/75% Water	21
e. Racemization: Effect of Temperature	22
f. Racemization: Effect of Residence Time	22
g. Racemization: 2.0 Equiv (-)-CSA	23
h. Solubility Curve: Time Course Data	23
i. Solubility Curve: Transparent Data Points for Error Bar Visualization	24
j. CIDT: Solids Transfer Uncorrected Data	24
k. CIDT: Racemization with Dissolver Flask Turbidity Trend	25
l. CIDT: Final Experiment Part 1 (Setup)	25
m. CIDT: Final Experiment Part 2 with Crystallizer Flask Turbidity Trend	26
8. PXRD Spectra	26
a. Enantiopure (-)-TBZ•(-)-CSA (3)	27
b. (-)-TBZ•(-)-CSA, ~0% e.e. (4)	27
c. Enantiopure vs. Racemic TBZ•(-)-CSA Comparison	27
d. (-)-TBZ•(-)-CSA, ~0% e.e. (unknown)	28
e. Racemic TBZ•(-)-CSA Comparison	29
9. Single Crystal XRD Data - (+)-TBZ•(-)-TBZ•2 (-)-CSA•2 H₂O	30
10. References	47

1. General Info

a. Chemical Suppliers

(-)-Camphorsulfonic acid was purchased from AK Scientific. Tetrabenazine was synthesized according to our previously described procedure.¹ *N,N*-diisopropylamine (DIPA) and HPLC-grade acetone were purchased from Sigma. Optima-grade ultra-high performance liquid chromatography solvents were purchased from Fisher. 6,7-dimethoxy-1,2,3,4-tetrahydro-quinoline hydrochloride salt and 3-[(dimethylamino)methyl]-5-methylhexan-2-one oxalate were supplied by Neurocrine Biosciences Inc. All other reagents and solvents were purchased from conventional suppliers and used as received unless otherwise stated.

b. Equipment Setup

All experiments were performed in Mettler-Toledo EasyMax 102 Advanced Thermostat System glass reactors (100 mL or 250 mL) equipped with Teflon reactor covers, submersible thermocouple, and a magnetic stir bar controlled by the Mettler-Toledo software iControl 6.1. The internal reactor temperature (T_r) was maintained by the EasyMax and measured by a thermocouple placed directly inside the reactor. The continuous multi-well CIDT setup made use of an EasyMax, IKA Plate, and two VapourTec SF-10 reagent pumps, connected via the minimum amount of IDEX ETFE 1/8" OD x 1/16" ID tubing. A custom-made inline racemization chamber was designed to have tubing coiled around it while fitting inside an EasyMax 102 reactor well. Filters were added to tubing drawing solution out of each reactor (i.e., lines leading to pump inlets) in order to prevent solids transfer between vessels.

Mettler-Toledo's iC Vision software was used in conjunction with a Mettler-Toledo EasyViewer probe for the acquisition of turbidity data and crystal images. A custom-built Python script was also used to obtain turbidity and solubility measurements using a webcam (see section SI 3 below). A Bruker D8-Advance X-ray diffractometer was used to obtain powder x-ray diffraction (PXRD) data. Temporal concentration data was obtained using a custom-built automation rig comprised of an EasySampler, diluent solvent pump, combined 6-port valve, solenoid valve and pressure sensor module (CombiValve) and an Agilent 1290 Infinity HPLC connected in series. A custom-built filter tip attachment was used to facilitate solution-phase exclusive sampling with the EasySampler.² Control of all components except the HPLC was carried out by a custom in-house built control module (DI Box) capable of triggering the EasySampler extension and retraction, pump operation and speed, valve positions, monitoring inline pressure, and sending a signal to trigger the collection of HPLC data. This DI Box controls all components necessary for direct injection of samples from the EasySampler onto the HPLC and is operated by means of a custom-built Python script and graphic user interface. Agilent's Chemstation program was used in conjunction with our DI Box to acquire and analyze samples as frequently as the sample run times would allow. Sampling events were controlled via third party software sending a signal at the requested sampling frequency (e.g. every 10 minutes) to our Python script, which would then carry out all of the necessary functions required to obtain the sample and transport it via diluent solvent to the HPLC. A normal sampling sequence with the running Python script looks like:

1. Third party software sends the signal to our Python script that it is time to begin the sampling sequence
2. The EasySampler is extended
3. The pump is started and pre-fills the lines with a specified volume of diluent solvent at a specified flow rate
4. The EasySampler is retracted
5. The 6-port valve position is changed such that the sample loop is now inline with the pump and EasySampler
6. The pump is started and pushes the sample through the lines into the inline sample loop on the 6-port valve
7. The 6-port valve position is changed such that the sample loop is now inline with the HPLC
8. A signal is sent from the DI Box to the HPLC (Chemstation) to begin data collection
9. The pump is started and the lines are washed with a specified volume of diluent solvent
10. The solenoid valve is actuated and an alternate solvent is selected
11. The pump is started and the lines are filled with the alternate solvent (such that extension of the EasySampler introduces 20 μL of this solvent and not diluent into the reaction)
12. The solenoid valve is actuated and returned to the diluent solvent position for the next sampling sequence
13. The third party software waits for a signal from Chemstation that the current HPLC run is over before sending the signal to begin the next run

Offline HPLC samples were acquired using a Microlit RBO 1000 μL micropipette, delivered into a Corning Costar Spin-X 0.45 μm Nylon centrifuge tube filter in a 2.0 mL polypropylene tube, and centrifuged using an Eppendorf Centrifuge 5417R.

c. Analytical Methods

PXRD data was acquired using a Bruker D8-Advance X-ray diffractometer in Bragg-Brentano configuration with Copper $K\alpha_1$ and $K\alpha_2$ radiation sources. A Nickel filter was used to filter out the $\text{CuK}\beta$ line. The detector was a LynxEye silicon strip and the generator was 40 kV and 40 mA. The slits used were 1 mm divergent, 8 mm anti-scatter and 2.5° soller. Samples were powder packed in a standard Bruker sample holder and were not rotated. Scans were plotted using HighscorePlus (Malvern-Panalytical).

HPLC analysis was performed on an Agilent 1290 Infinity HPLC equipped with DAD detector. The collected samples were analyzed at 285 nm using the following chiral method:

Daicel IC-3 Chiralpak Column, 2.1 x 150 mm; 3 μm

Solvent A = Water; Solvent B = Methanol (0.1 % DIPA v/v)

Flow Rate = 0.450 mL/min

Column Temperature = 35 °C

Sample Loop Volume = 100 μL

Gradient: A:B 15:85 – initial (isocratic)

9 min stop time, no post time

With the above method, (-)-TBZ and (+)-TBZ could be resolved from one another as well as the from the diastereomer resulting from epimerization α to the ketone of (-)-TBZ (the diastereomer of (-)-TBZ). However, the analogous diastereomer of (+)-TBZ could not be resolved from the (+)-TBZ peak and presented itself as a broadening of the peak when the other diastereomer peak was observed. Since this resulted in (-)-TBZ being the only enantiomer that could be fully resolved from all other components, and since racemization studies were necessary to develop a CIDT reaction, (-)-CSA was chosen as the chiral resolving agent in order to obtain enantiopure (-)-CSA•(-)-TBZ. As such, this gave us access to enantiopure (-)-TBZ after removing the chiral resolving agent, instead of (+)-TBZ which is the biologically active enantiomer.

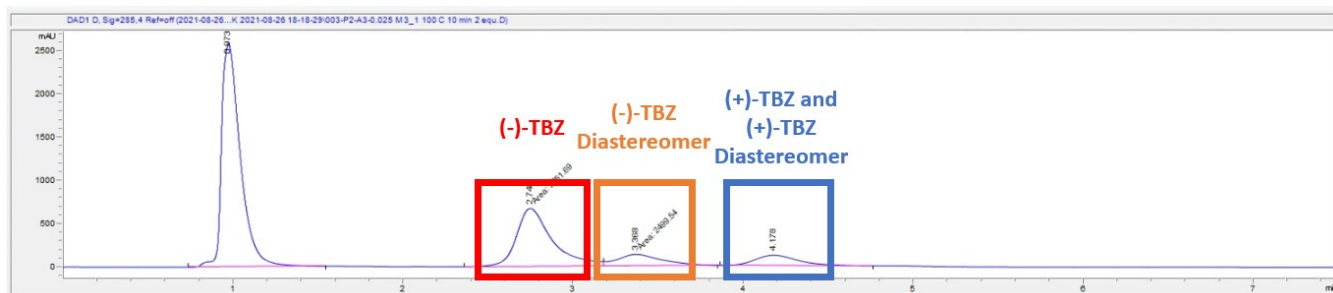


Figure SI 1. Sample chiral HPLC chromatogram illustrating resolution of (-)-TBZ and its diastereomer but overlapping (+)-TBZ and diastereomer peaks.

2. System Hardware and Configurations

a. VapourTec Flow System

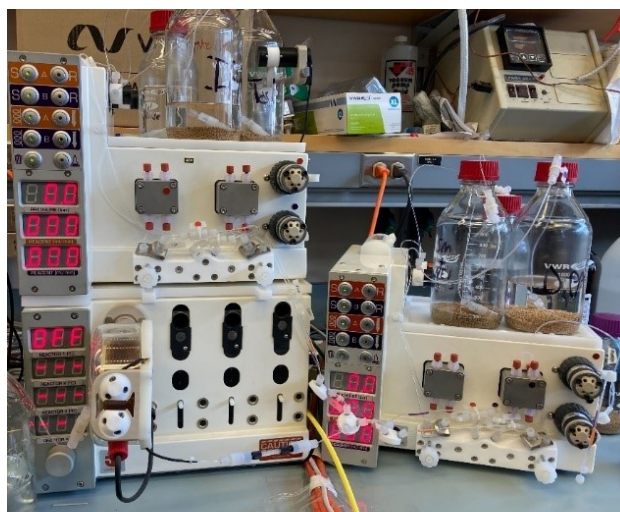


Figure SI 2. Customized VapourTec flow system comprised of one R4 reactor heater module (bottom middle) and two R2C+ pump modules (top middle and bottom right). Analyte solution was pumped through the 10 mL reactor loop while flow rate and temperature were varied in order to determine the effects of reactor temperature and residence time on racemization and decomposition.

b. CIDT System – Configuration #1



Figure SI 3. Continuous multi-well CIDT system flow path, showing pumping direction: starting in the warm dissolver flask at room temperature (24 °C, yellow), solution was pumped through pump #1 to the cold crystallizer flask (variable temperature, blue), then through pump #2 and through the inline racemization chamber (100 °C) before being returned to the dissolver flask. In this configuration, the temperature of the warm dissolver flask could not be adjusted (being static at room temperature) and a webcam was used to monitor the dissolver and crystallizer flasks. A 20 PSI back pressure regulator was installed to allow temperatures greater than the boiling point to be reached, allowing the solution to be heated to 100 °C for racemization.



Figure SI 4. Continuous multi-well CIDT system analytics, with webcams (for turbidity measurements) and EasySampler (for online HPLC solution phase concentration measurements) highlighted. Solution phase aliquots were delivered to the HPLC via a system of tubing, valves and pumps (not highlighted). A cardboard enclosure was installed around the dissolver flask (left) to minimize the effects of external lighting on the extracted turbidity trends, and a cooling fan was added to ensure room temperature was maintained.

c. CIDT System – Configuration #2

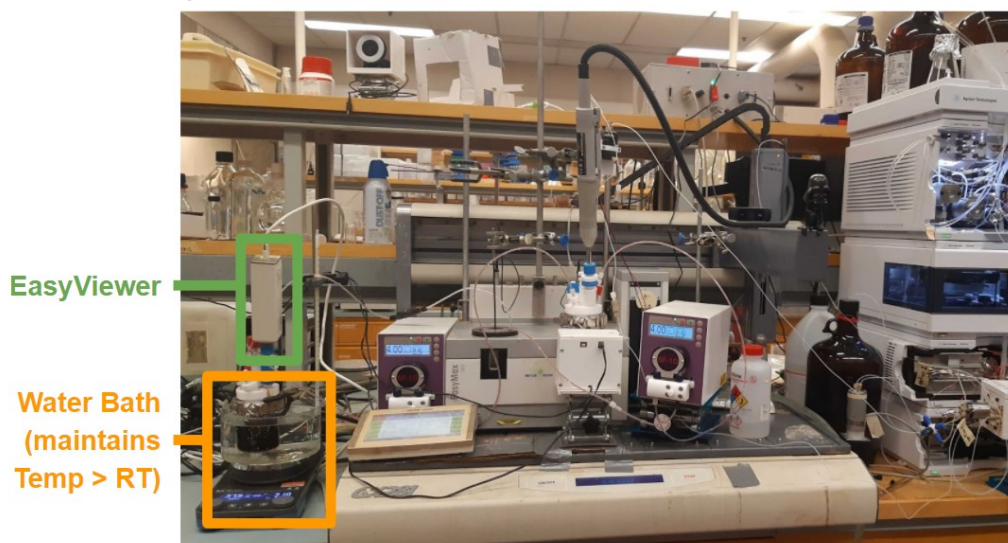


Figure SI 5. Updated continuous multi-well CIDT configuration using water bath and EasyViewer instead of cardboard enclosure and webcam, allowing for warm dissolver flask to be maintained at temperatures higher than room temperature (RT) while still allowing turbidity measurements to be acquired (using the EasyViewer instead of the webcam and enclosure).

d. Inline Racemization Chamber



Figure SI 6. Inline racemization chamber consisting of two coils of 1/8" OD x 1/16" ID IDEX ETFE tubing wrapped around a 3D printed cylinder. Final model was printed using Formlabs high temperature resin. Grooves keep tubing in place such that the assembly can be inserted inside the reactor well of an EasyMax 102 Advanced Thermostat unit. Total tubing volume was 7.4 mL between pump #2 and the 20 PSI backpressure regulator located after the coil to allow elevated temperatures for racemization. The chamber contains two coils of tubing (one nestled underneath the other), each with a pitch of 10 turns over 5.0 cm. Inner coil diameter (D_c) is 5.06 cm ($D_c/ID = 1.62$), outer coil diameter is 5.7 cm ($D_c/ID = 1.82$).

3. Webcam Turbidity Measurements

a. Software

Our lab developed a custom-built Python script that uses a webcam to acquire images and processes their relative brightness (compared with a specified “region of interest”) to determine the turbidity of a solution. Coworkers Veronica Lai and Dr. Tara Zepel previously demonstrated this script’s ability to determine a compound’s solubility when combined with a robotic platform.³ In the current study, the script was combined with Mettler-Toledo’s iControl software to determine a compound’s solubility on larger scales than previously demonstrated (i.e., gram scale compared with milligram scale). This was achieved by importing our algorithm’s turbidity data into the Mettler-Toledo iC Vision software, from which it could be processed in iControl for experimental design and automated feedback.

b. Hardware

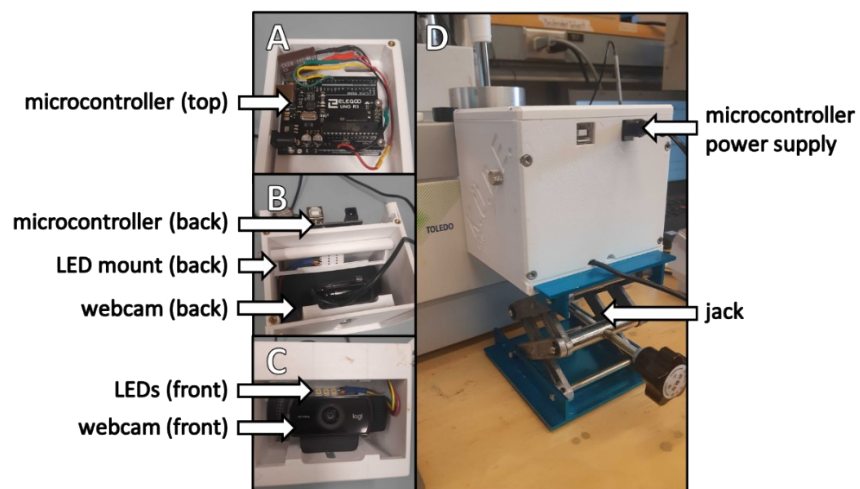


Figure SI 7. Webcam enclosure comprised of 3D printed box (white) in various orientations: A) top internal orientation showing microcontroller; B) back orientation showing microcontroller, LED mount and back of webcam; C) front orientation showing webcam and LEDs on LED mount; D) apparatus installed on a jack in front of an EasyMax being used to monitor reactor turbidity.

A custom-built 3D printed enclosure was designed to block out external light and supply a constant source of illumination to minimize noise in the computer-vision webcam turbidity data. Constant illumination was provided by LEDs modulated by a microcontroller. The apparatus was designed to rest on a jack so that its height in front of a reactor (in this case, a Mettler-Toledo EasyMax reactor well) could be adjusted to optimize image quality.

c. Automated Solubility Curve iControl Procedure

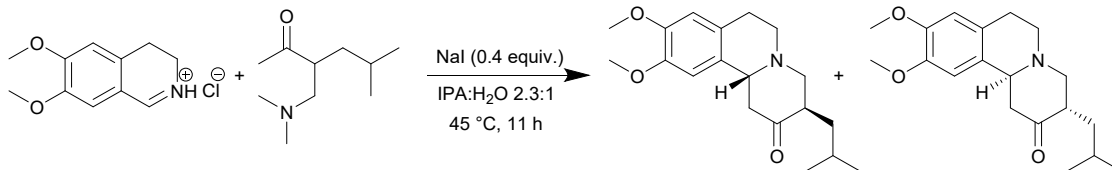
Using our custom-built Python script and Mettler-Toledo's iControl and iC Vision software, we performed automated feedback experiments that autonomously obtained a solubility curve for the chosen compound and solvent system. Our procedure (outlined below in SI section 6b) used the following iControl procedure to automatically determine the clear point (and thus, the solubility) of the chosen compound at a variety of concentrations. The script required a dissolved turbidity value ($X_{\text{dissolved}}$) associated with the clear point (i.e. total compound dissolution), and a threshold turbidity value (X_{solids}) associated with the presence of sufficient solids to increase the temperature and make another clear point measurement. This setup required an EasyMax with an external dosing unit to deliver the chosen into the reactor. The iControl procedure was as follows:

1. Cool reactor to 2 °C at 0.5 K/min, but end early if turbidity > X_{solids}
2. Wait until turbidity > X_{solids} (confirms that enough solids are present for clear point measurement)
3. Heat reactor to 60 °C at 0.5 K/min, but end early if turbidity < $X_{\text{dissolved}}$
4. Wait until turbidity < $X_{\text{dissolved}}$ (confirms that solids have fully dissolved)
5. Dose 5 mL of chosen solvent (e.g., a 75-25 acetone-water mixture) into the reactor
6. Wait 60 minutes for mixing and/or further dissolution
7. Repeat the cycle

After termination of the experiment (either manually if nucleation was determined to be too slow, or automatically if the reactor volume limit was reached), another script automatically abstracted the clear point values and calculated the solution concentrations based on the initial volumes.

4. Synthetic Procedures

a. Tetrabenazine (TBZ)



To a 100 mL EasyMax flask equipped with a stir bar were added isopropyl alcohol (IPA; 20.4 mL), water (8.8 mL), 3-[(dimethylamino)methyl]-5-methylhexan-2-one (5.48 g, 32.00 mmol, 1.25 equiv.), 6,7-dimethoxy-1,2,3,4-tetrahydroquinoline hydrochloride salt (5.83 g, 25.60 mmol, 1.00 equiv.), and NaI (1.53 g, 10.24 mmol, 0.40 equiv.). The mixture was stirred vigorously for 11 hours at 45 °C. 12 mL of water was then added to the mixture at 0.1 mL/min, after which the mixture was cooled to 5 °C at 0.1 K/min. The mixture was filtered to afford tetrabenazine (4.58 g, 56.3%) as a white crystal. ¹H NMR (400 MHz, CDCl₃) δ 6.62 (s, 1H), 6.55 (s, 1H), 3.86 (s, 3H), 3.83 (s, 3H), 3.51 (dd, *J* = 11.8, 2.9 Hz, 1H), 3.29 (dd, *J* = 11.5, 6.3 Hz, 1H), 3.19 – 3.05 (m, 2H), 2.90 (dd, *J* = 13.6, 3.1 Hz, 1H), 2.81 – 2.67 (m, 2H), 2.64 – 2.49 (m, 2H), 2.36 (t, *J* = 11.6 Hz, 1H), 1.80 (ddd, *J* = 13.9, 8.5, 5.5 Hz, 1H), 1.66 (ddt, *J* = 12.9, 8.5, 6.5 Hz, 1H), 1.04 (ddd, *J* = 13.6, 7.4, 5.8 Hz, 1H), 0.92 (appt dd, *J* = 6.6, 4.7 Hz, 6H); ¹³C NMR (100 MHz, CDCl₃) δ 210.1, 147.9, 147.6, 128.5, 126.1, 111.5, 107.9, 62.5, 61.5, 56.1, 56.0, 50.7, 47.6, 47.5, 35.1, 29.4, 25.5, 23.3, 22.2; MS ESI⁺ (calc. for C₁₉H₂₇NO₃, 317.20): *m/z* = 318.2 [M+H]⁺.

b. Enantiopure (-)-TBZ·(-)-CSA (**3**)

See SI section 6g for CIDT procedure yielding enantiopure (-)-TBZ·(-)-CSA via controlled crystallization.

c. (-)-TBZ·(-)-CSA (**3**), 70% e.e.

The following procedure was adapted from Yao et al.⁴ using (-)-CSA instead of (+)-CSA, in an attempt to synthesize enantiopure (-)-TBZ·(-)-CSA:

To a 100 mL rbf equipped with stir bar was added racemic TBZ (2.98 g, 9.39 mmol, 1.00 equiv) and (-)-CSA (2.18 g, 9.39 mmol, 1.00 equiv). Reagent grade acetone (25 mL) was then added and the solution refluxed for 16 hours. The solution was then cooled to room temperature and filtered via suction filtration to afford scalemic (-)-TBZ·(-)-CSA (2.21 g, 85% yield, 65% e.e.).

d. (-)-TBZ·(-)-CSA, ~0% e.e. (**4**)

To a 40 mL vial equipped with stir bar was added enantiopure (-)-TBZ·(-)-CSA (549 mg, 1.00 mmol) and 40 mL isopropanol. The reaction was heated to 80 °C for 18 h stirring at 300 rpm, then solvent was evaporated via airflow to afford near-racemic solids (8% e.e.). **4** was also crystallized in the warm dissolver flask during the final CIDT experiment due to hardware failure (see SI sections 6g and 7l below).

5. Calibration and Standard Additions

a. Background

While the analytes' molar absorptivities were not expected to change between experiments, significantly altering the analyte concentration, chiral resolving agent concentration, solvent composition and/or presence of decomposition products (taken together as 'matrix effects') risked changing the chromatographic separation and/or detector response for TBZ. As a traditional calibration curve performed separate from experimental data acquisition cannot account for all such possible changes, standard additions were determined to be the best method to obtain reliable concentration data. Consequently, standard additions were performed at the beginning of each online HPLC experiment in order to calibrate the acquired concentration data.

b. Procedure

At the start of every experiment, at least two solvent blanks were acquired using online HPLC. TBZ was then added in no less than two portions such that both portions completely dissolved, resulting in an experiment-specific calibration curve with at least two data points. The slope of this calibration curve could then be used to convert all raw peak area values from the online HPLC data into concentration data, allowing analyte concentration vs. time to be plotted.

c. Sample Raw Data – Solubility Curve Experiment

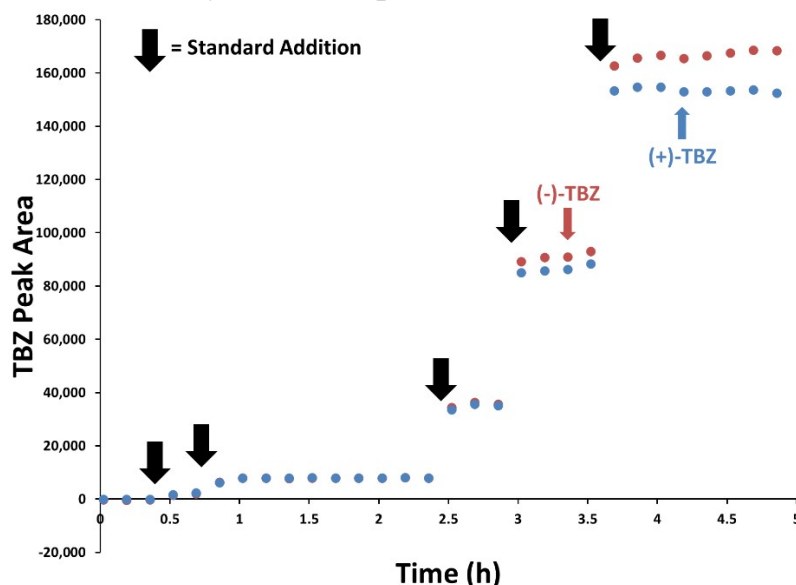


Figure SI 8. Sample standard addition raw data from beginning of solubility curve experiment with 2.0 equiv of (-)-CSA (prior to time = 0 h). Increasing standard additions are noted with black arrows: 90.6 mg, 204.0 mg, 976.5 mg, and 2.010 g of racemic TBZ were added after two initial solvent blanks at 0.5 h.

d. Sample Calibration Curves – Solubility Curve Experiment

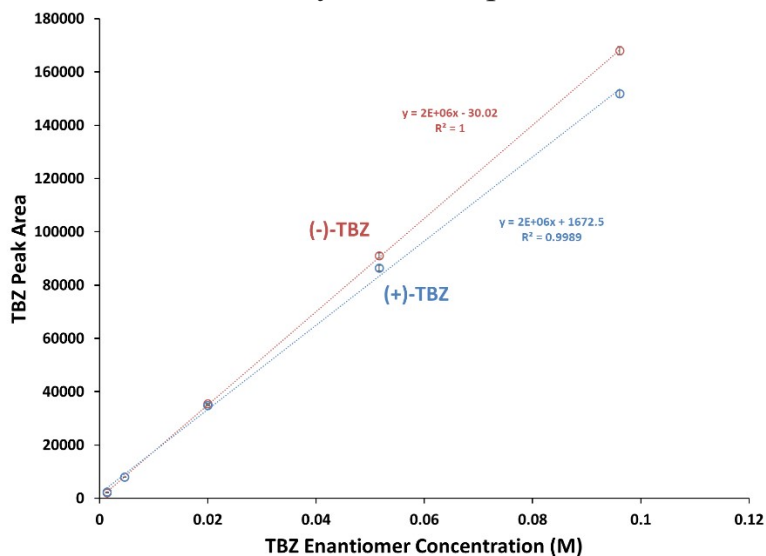


Figure SI 9. Calibration curves generated by averaging standard addition raw data signals after peak area (from Figure SI 8) was observed to plateau. Standard deviations are shown as error bars for each data point, with transparent data points allowing the error bars to be seen due to their small size.

6. Experimental Procedures

a. General Manual Sampling Procedure

Manual solid and solution phase sampling were performed using a micropipette and a centrifuge. Before taking a sample, the lower 3 mm of a 1 mL micropipette tip was removed to allow larger particles to be sampled than would otherwise be possible. To take the sample, ~500 μ L of solution (no longer calibrated precisely due to the change in tip geometry) was transferred to a centrifuge vial with a micropipette. This sample was immediately transferred to a centrifuge preheated to the same temperature as the reaction solution (to prevent undesired dissolution and/or solid nucleation) and centrifuged at 9000 rpm for 3 minutes. After centrifugation, the solids were dissolved in ~500 μ L MeOH, transferred to an HPLC vial and diluted to ~1 mL, while the solution phase was transferred to a separate HPLC vial and diluted to ~1 mL with MeOH. Both vials were then submitted for offline chiral HPLC analysis to determine each phase's e.e.

b. General Automated Solubility Curve Procedure – Figure 3 and Figure SI 10-13

To a 100 mL EasyMax flask equipped with a stir bar was added the chosen solvent (50 mL). The solution was raised to 10 °C lower than the mixture's boiling point or the boiling point of the most volatile component (whichever was lower), and stirred at 200 rpm. (-)-TBZ•(-)-CSA (**3**) was then added in 500 mg portions until dissolution was no longer observed. The temperature was increased until the compound fully dissolved, after which point the iControl automated feedback procedure was performed (see above SI section 3c) until the maximum reactor volume (120 mL) was reached or nucleation was no longer observed (or too slow to be detected by our analytics). The data from experiments with different solvent compositions was combined to create Figure 3 using the temperature closest to 25 °C from each solubility curve.

c. General VapourTec Racemization Procedure – Figure 4 and Figure 14-16

A solution of (-)-TBZ•(-)-CSA was prepared in 75% acetone/25% water at the desired concentration. This solution was then used to fill two tubing lines into both reagent pump channels on a Vapourtec R2 pump and joined by a T mixer to a 10 mL reactor on a R4 heater module. The solvent pump channels were connected to a solution of 75% acetone/25% water. The Vapourtec R4 reactor heater was set to the desired experiment temperature (maximum 150 °C). The combined flow rate of both channels on the R2 pump was set to give the desired residence time at a backpressure of ~16 bar. The reactor was first flushed with solvent for two residence times, then switched to the analyte solution. After flowing the analyte solution for three residence times to allow for equilibration, 1 mL of solution was then collected and submitted for chiral offline HPLC analysis. The system was then switched back to 75% acetone/25% water and flushed in preparation of the next experiment.

d. Solubility Curve Procedure – Figure 6 and Figure SI 8, 9, 17 and 18

To a 100 mL EasyMax flask equipped with stir bar was added 75 mL of acetone and 25 mL of DI water. The solution was stirred at 200 rpm and heated to a reactor temperature of 45 °C. Online HPLC solution phase sampling was initiated (at a rate of one sample every 10 minutes) and three solvent blanks were acquired. TBZ was then added in a series of standard additions, during which the solids rapidly dissolved and the solution returned to homogeneous: 90.6 mg, 204.0 mg, 976.5 mg, and 2.010 g were added. At least three samples were acquired during each standard addition. An additional 2.82 g of TBZ was then added (for a total of 6.10 g TBZ, 19.2 mmol, 1.0 equiv) along with (-)-CSA (8.93 g, 38.4 mmol, 2.0 equiv). The solution was then cooled to 5 °C to induce solid nucleation and sampled for 3 hours to monitor crystallization. Lastly, the solution was heated in 5 °C stepwise increments up to 45 °C to obtain solubility data at these temperatures.

The reactor failed to maintain the set temperature twice (first at 20 °C and then 30 °C), visible as the reactor temperature dropped to the temperature of the coolant solution (16.5 °C) before being reset and the procedure resumed.

e. CIDT: Solids Transfer Procedure – Figure 7, Figure SI 19

To two 100 mL EasyMax flasks equipped with stir bars was added 90 mL of 75% acetone/25% water, for a total of 180 mL. The system was setup according to configuration #1 (see SI section 2b above), with the cold crystallizer flask cooling to 15 °C, the warm dissolver flask constant at ambient temperature (24 °C) and the inline racemization chamber maintained at 25 °C. The reactors were stirred at 300 rpm, and the pumps were run at 2 mL/min for 1 hour to circulate solvent throughout the system and prepare the lines. Racemic TBZ (6.10 g, 19.2 mmol, 1.0 equiv) and (-)-CSA (8.93 g, 38.4 mmol, 2.0 equiv) were then added to the warm dissolver flask to make a heterogeneous solution, and pumping between the solutions continued for 2 hours to fully equilibrate the system. No solids nucleation was observed in the cold dissolver flask, so online HPLC measurements were begun (sampling every 15 minutes). After 30 minutes, 200 mg of enantiopure (-)-TBZ•(-)-CSA was added to the cold crystallizer flask as seed crystals and the flask immediately became cloudy. 50 minutes later, webcam turbidity measurements were started, and the warm dissolver flask was observed to become homogeneous (i.e., all solids had dissolved) by 6 hours. Manual sampling after 14 hours indicated solids in the cold crystallizer flask were enantiopure (-)-TBZ•(-)-CSA (>99% e.e.), the solution phase of the cold crystallizer flask was -26% e.e. and the solution phase of the warm dissolver flask was -28% e.e. This closely matched the online HPLC data, which indicated both solutions should have -33% e.e., suggesting our online HPLC data was accurate (as manual sampling would inevitably dissolve some of the enantiopure (-)-TBZ•(-)-CSA, skewing the e.e. slightly more positive). The solids and solution from this experiment were not isolated, being used directly in another experiment.

f. CIDT: Racemization Procedure – Figure 4, Figure SI 20

To two 100 mL EasyMax flasks equipped with stir bars was added 80 mL of 75% acetone/25% water, for a total of 160 mL. The system was setup according to configuration #2 (see SI section 2c above), with the cold crystallizer flask cooling to 15 °C, the warm dissolver flask held at 30 °C, and the inline racemization chamber initially maintained at 25 °C. The reactors were stirred at 300 rpm, and the pumps were run at 2 mL/min for 30 minutes to circulate solvent throughout the system and prepare the lines. Racemic TBZ (6.10 g, 19.2 mmol, 1.0 equiv) and (-)-CSA (8.93 g, 38.4 mmol, 2.0 equiv) were then added to the warm dissolver flask to make a heterogeneous solution that became homogeneous after ~1 hour. Pumping between the solutions continued for 1.5 hours to fully equilibrate the system. The cold flask was observed to have solids present, indicating that uncontrolled nucleation had occurred. As such, the cold flask was heated to 30 °C to dissolve the solids, at which point online HPLC measurements were begun (sampling every 15 minutes) and the cold flask was cooled back to 15 °C. After 1 hour, 200 mg of enantiopure (-)-TBZ•(-)-CSA was added to the cold crystallizer flask as seed crystals and the flask immediately became cloudy. Lastly, the inline racemization chamber was heated to approximately 100 °C to begin racemization. After 15 hours, manual sampling indicated that the cold crystallization flask contained enantiopure (-)-TBZ•(-)-CSA (>98% e.e.) and the solution phase of both flasks were nearly racemic (with the cold and warm flasks being 2% e.e. and 0.6% e.e., respectively). The solids and solution from this experiment were not isolated, being used directly in another experiment.

g. CIDT: Final Experiment Procedure – Figure 9 and Figure SI 21 and 22

Part 1 (data before Figure 9):

To two 100 mL EasyMax flasks equipped with stir bars was added 100 mL of 75% acetone/25% water, for a total of 200 mL. The system was setup according to configuration #2 (see SI section 2c above), with the cold crystallizer flask initially cooling to 15 °C, the warm dissolver flask held at 33 °C, and the inline racemization chamber initially maintained at 25 °C. Racemic TBZ (5.10 g, 16.1 mmol, 1.0 equiv) and (-)-CSA (8.20 g, 35.3 mmol, 8.20 equiv) were added to the warm dissolver flask, and it was stirred for 3 hours at 33 °C to equilibrate the mixture (which dissolved). At the same time, online HPLC measurements were begun in the cold crystallizer flask (sampling once every 15 minutes). After 1 hour of acquiring solvent blanks at 15 °C, racemic TBZ (503 mg, 1.58 mmol, 1.0 equiv) and (-)-CSA (368 mg, 1.58 mmol, 1.0 equiv) were added to the cold flask as the first standard addition, and the solution sampled for another hour. An additional standard addition of racemic TBZ (501 mg, 1.58 mmol, 1.0 equiv) and (-)-CSA (366 mg, 1.58 mmol, 1.0 equiv) was then added and the solution again sampled for an hour. Webcam and EasyViewer turbidity measurements were started, and the pumps started at 2 mL/min to circulate solution between the flasks. The cold flask was temporarily heated to 30 °C to ensure no solids were present, and the inline racemization chamber was heated to 100 °C. The cold flask was then cooled back to 15 °C and 200 mg of enantiopure (-)-TBZ•(-)-CSA was added to the cold crystallizer flask as seed crystals at 6 hours, at which point the solution immediately became cloudy. 15 hours later, manual sampling confirmed that the solids in the cold flask were enantiopure (>98% e.e.). Racemic TBZ (1.587

g, 5.0 mmol, 1.0 equiv) and (-)-CSA (1.161 g, 5.0 mmol, 1.0 equiv) were added to the warm dissolver flask at 21 h, which immediately became homogeneous again. To avoid unwanted solids nucleation, the cold dissolver flask was increased to 25 °C for the remainder of the experiment. After 24 hours, racemic TBZ (1.587 g, 5.0 mmol, 1.0 equiv) and (-)-CSA (1.161 g, 5.0 mmol, 1.0 equiv) were each added to the warm dissolver flask three times: first at 46 h, then again at 48.5 h, and then again at 51 h. The system was run for another 20 h, with a minor hardware failure at 61 h quickly corrected. Racemic TBZ (1.587 g, 5.0 mmol, 1.0 equiv) and (-)-CSA (1.161 g, 5.0 mmol, 1.0 equiv) were added to the warm dissolver flask at 71 h, and the system run another 27 h. Another minor hardware failure occurred at 81 h and was corrected at 88 h. Manual sampling at 98 h confirmed that the cold crystallizer flask contained enantiopure (-)-TBZ•(-)-CSA (>98% e.e.). The online HPLC and turbidity measurements were stopped and restarted to prevent file sizes from becoming unmanageable.

Part 2 (Figure 9, and afterwards):

Racemic TBZ (1.587 g, 5.0 mmol, 1.0 equiv) and (-)-CSA (1.161 g, 5.0 mmol, 1.0 equiv) were added to the warm dissolver flask at 0 h, 19 h, and 67 h based on online HPLC data. Additions were only performed once racemization dropped the (+)-TBZ concentration below 0.09 M in order to avoid undesired racemic TBZ solids formation. At 123 h, hardware failure resulted in the cold reactor flask rapidly heating, dissolving enantiopure (-)-TBZ•(-)-CSA and depositing racemic TBZ•(-)-CSA solids in the warm dissolver flask. Cold solids were isolated by suction filtration, washing with 10 mL of 75% acetone/25% water to provide 10.35 g of (-)-TBZ•(-)-CSA (>98% e.e.). The filtrate was replaced within the cold crystallizer flask and the solution circulated again at 2 mL/min. After multiple hardware failures, 200 mg of enantiopure (-)-TBZ•(-)-CSA was added to the cold crystallizer flask as seed crystals and racemic TBZ (1.587 g, 5.0 mmol, 1.0 equiv) and (-)-CSA (1.161 g, 5.0 mmol, 1.0 equiv) were added to the warm dissolver flask. One day later, more racemic TBZ (1.587 g, 5.0 mmol, 1.0 equiv) and (-)-CSA (1.161 g, 5.0 mmol, 1.0 equiv) were added. After 24 h, final solids isolated by suction filtration were 8.05 g of (-)-TBZ•(-)-CSA (>98% e.e.), for a total yield of 18.39 g of enantiopure (-)-TBZ•(-)-CSA (33.5 mmol, 48% yield). The filtrate and solution phase from the warm dissolver flask were combined and solvent removed *in vacuo*. The solids were added to DCM (100 mL) and 1.0 M NaOH (100 mL), and dissolved after stirring for 1 h. The organic phase was dried over anhydrous Na₂SO₄ and solvent removed *in vacuo* to afford 10.75 g of scalemic TBZ (-24% e.e.). Based on HPLC chiral resolution, this was composed of 4.09 g of (-)-TBZ, indicating that (-)-TBZ composed at least 67% of the system and that the CIDT was therefore a success.

Note on hardware failures: Our EasyMax 102 Advanced Thermostat System encountered errors after prolonged periods of maintaining the same temperatures, as required during this experiment. When this occurred, the cold reactor flask and inline racemization chamber would usually revert to the temperature of the coolant solution used within the EasyMax (16 °C), resulting in rapid crystallization in the cold crystallizer flask previously at 25 °C. This could be easily corrected by returning the crystallizer to 25 °C. However, at 123 h in Part 2, the system began to heat above 60 °C because of a failure. This dissolved some of the enantiopure (-)-TBZ•(-)-CSA in the crystallizer flask and caused undesired racemic solids to crystallize rapidly in the 33 °C dissolver flask, and is outlined in red in Figure 9.

7. Additional Experimental Data

a. (-)-TBZ•(-)-CSA Solubility in 100% Acetone

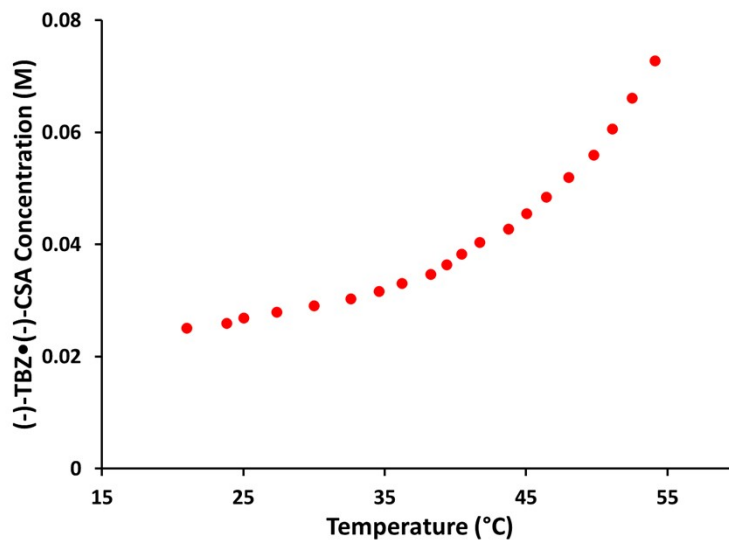


Figure SI 10. Solubility curve for (-)-TBZ•(-)-CSA in 100% acetone, automatically generated using webcam turbidity and iControl functionality from 2.00 g (-)-TBZ•(-)-CSA in 50.0 mL acetone.

b. (-)-TBZ•(-)-CSA Solubility in 75% Acetone/25% Water

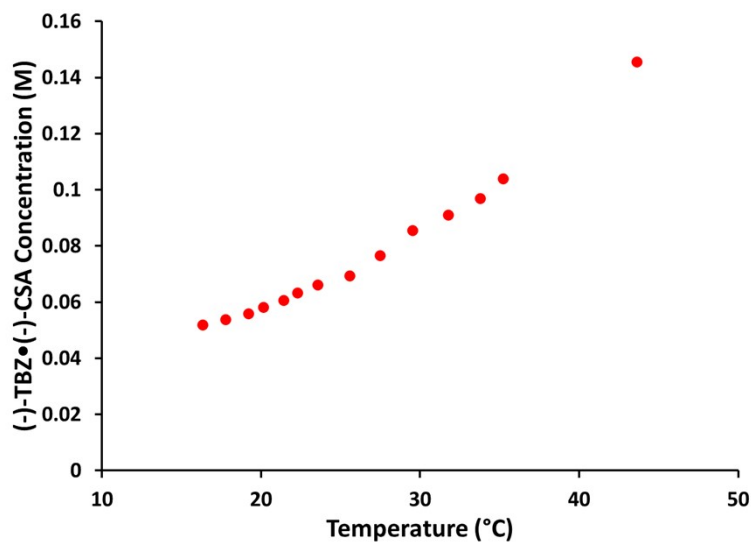


Figure SI 11. Solubility curve for (-)-TBZ•(-)-CSA in 75% acetone/25% water, automatically generated using webcam turbidity and iControl functionality from 4.00 g (-)-TBZ•(-)-CSA in 50.0 mL acetone. Outlier data points were discarded that due to incomplete dissolution.

c. (-)-TBZ•(-)-CSA Solubility in 50% Acetone/50% Water

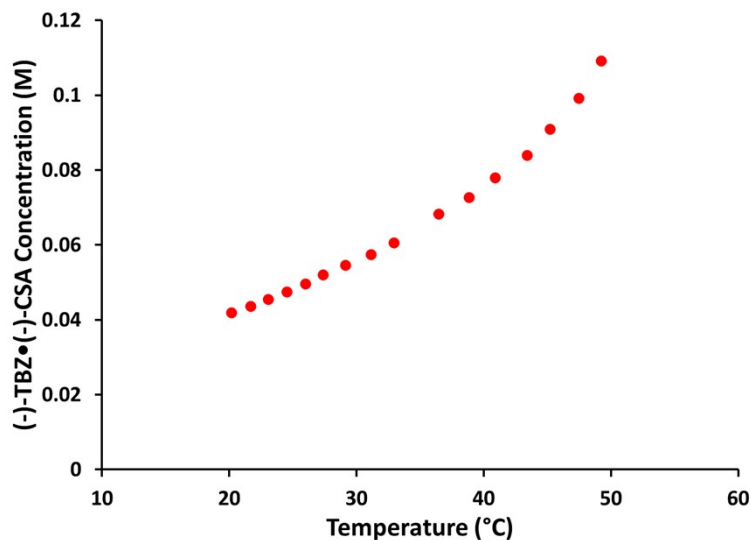


Figure SI 12. Solubility curve for (-)-TBZ•(-)-CSA in 50% acetone/50% water, automatically generated using webcam turbidity and iControl functionality from 3.00 g (-)-TBZ•(-)-CSA in 50.0 mL acetone.

d. (-)-TBZ•(-)-CSA Solubility in 25% Acetone/75% Water

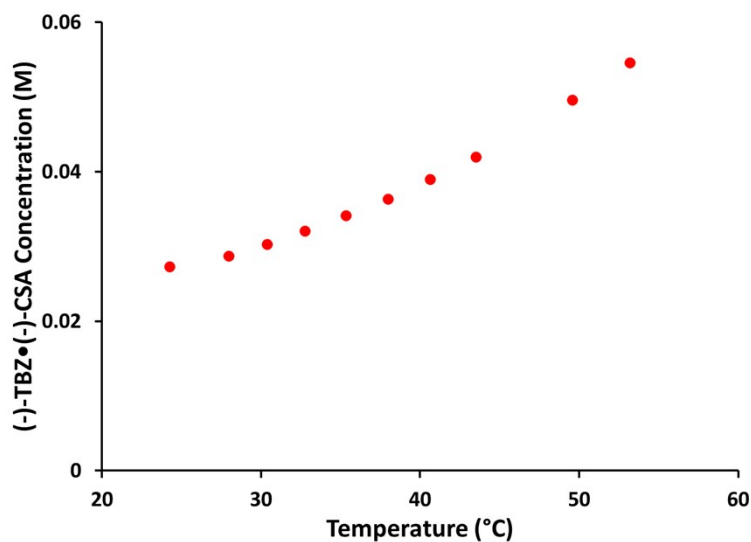


Figure SI 13. Solubility curve for (-)-TBZ•(-)-CSA in 25% acetone/75% water, automatically generated using webcam turbidity and iControl functionality from 1.50 g (-)-TBZ•(-)-CSA in 50.0 mL acetone.

e. Racemization: Effect of Temperature

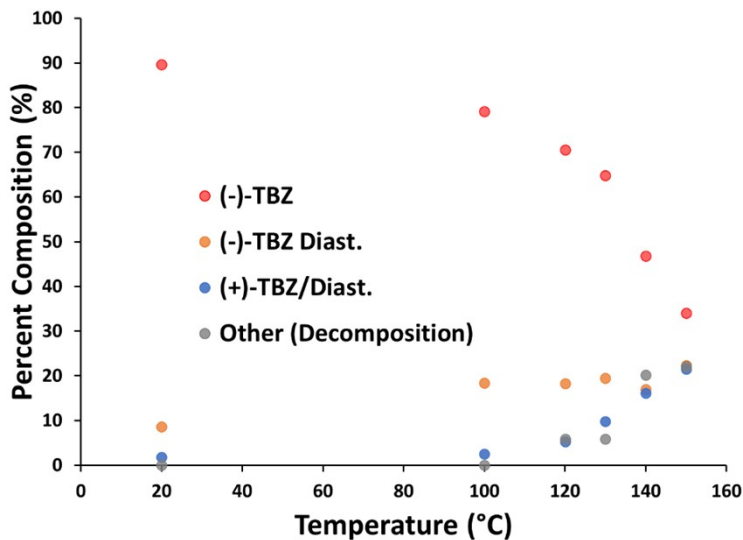


Figure SI 14. Change in percent composition as a result of flowing a 0.010 M (-)-TBZ•(-)-CSA solution in 75% acetone/25% water through the VapourTec flow system at various temperatures with a 10 minute residence time.

f. Racemization: Effect of Residence Time

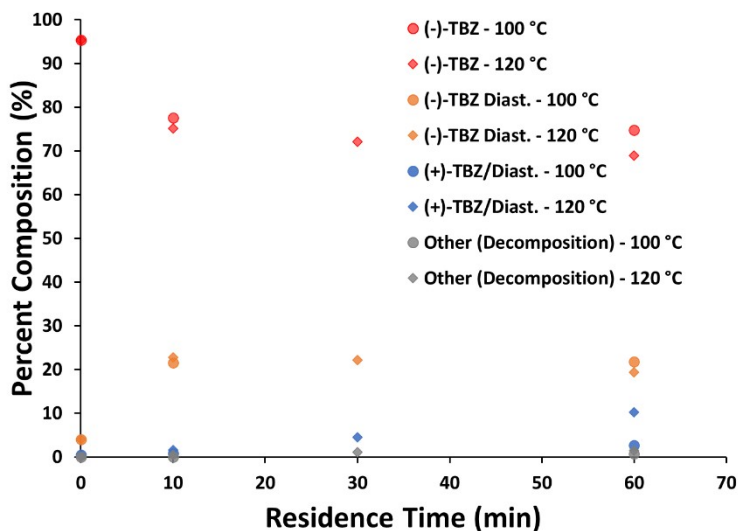


Figure SI 15. Change in percent composition as a result of flowing a 0.025 M (-)-TBZ•(-)-CSA solution in 75% acetone/25% water through the VapourTec flow system at various temperatures and residence times.

g. Racemization: 2.0 Equiv (-)-CSA

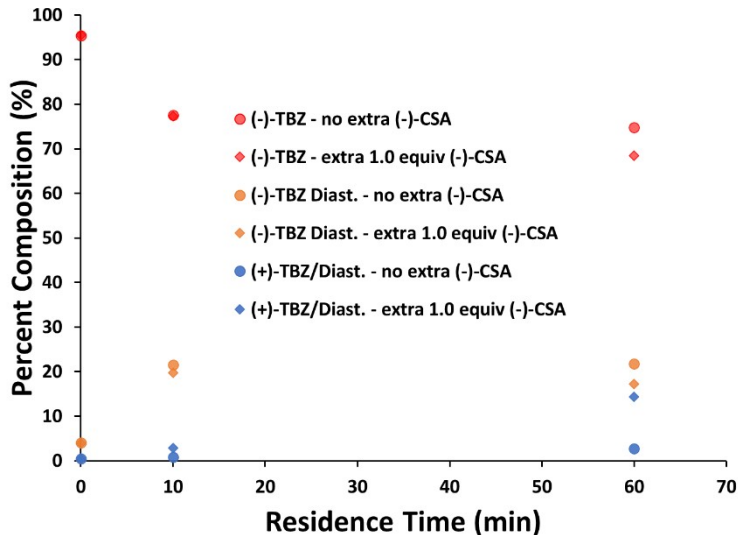


Figure SI 16. Change in percent composition as a result of flowing a 0.025 M (-)-TBZ•(-)-CSA solution with an extra 1.0 equiv of (-)-CSA (total 2.0 equiv) in 75% acetone/25% water through the VapourTec flow system at various residence times at 100 °C.

h. Solubility Curve: Time Course Data

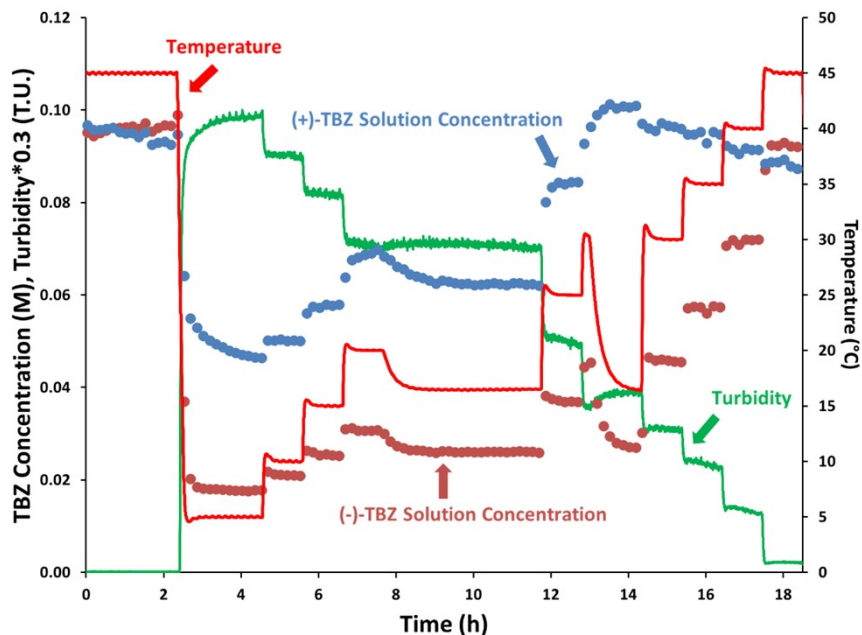
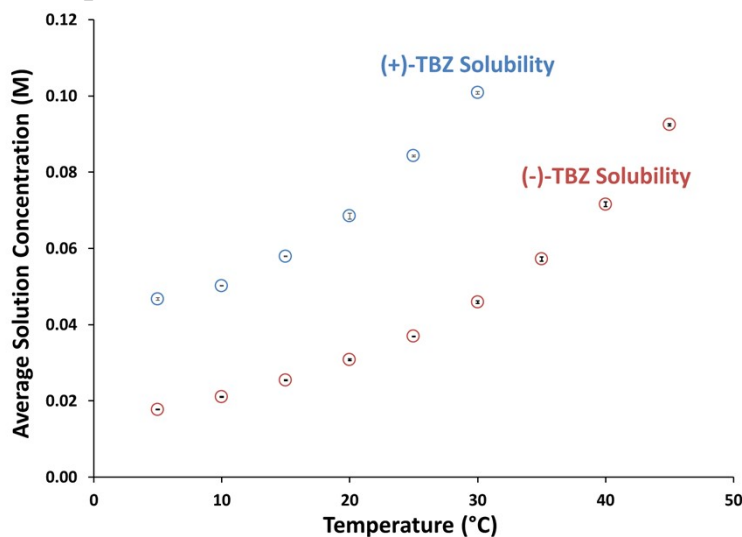


Figure SI 17. Time course online HPLC data for racemic TBZ solubility curve with 2.0 equiv of (-)-CSA. Total concentration was 0.096 M TBZ and 0.192 M (-)-CSA in 75% acetone/25% water. Initial standard additions are not shown (see Figure 6 and Figure SI 18).

i. Solubility Curve: Transparent Data Points for Error Bar Visualization



Temperature (°C)	(-)-TBZ Conc (M)	(+)-TBZ Conc (M)	(-)-TBZ Std Dev	(+)-TBZ Std Dev	RSD (-)-TBZ	RSD (+)-TBZ
45	0.096092461	0.094876854	0.001085838	0.001407	1.129993	1.482519
5	0.017733713	0.046740956	6.268E-05	0.000324	0.353451	0.693682
10	0.021045282	0.050213745	9.28911E-05	0.000112	0.441387	0.222793
15	0.025415343	0.057913343	0.000149267	0.000107	0.587312	0.185457
20	0.030823228	0.068475874	0.000233289	0.000794	0.75686	1.15958
25	0.03692357	0.084286875	4.02059E-05	0.000229	0.108889	0.271481
30	0.04592291	0.100847133	0.000354706	0.000333	0.772393	0.330472
35	0.057202624		0.000566217		0.989845	
40	0.071568836		0.000608056		0.84961	
45	0.092445241		0.000308767		0.334	

Figure SI 18. Concentrations of (+)-TBZ and (-)-TBZ obtained from Figure SI 17 were averaged for each temperature region (5 – 45 °C, in 5 °C increments) and plotted against temperature to obtain solubility curves for each TBZ enantiomer. Average values from multiple samples at each temperature are recorded, with the mean values being plotted. Relative standard deviation in these data points were no greater than 1.5% with an average RSD being 0.65% across all typical experiments.

j. CIDT: Solids Transfer Uncorrected Data

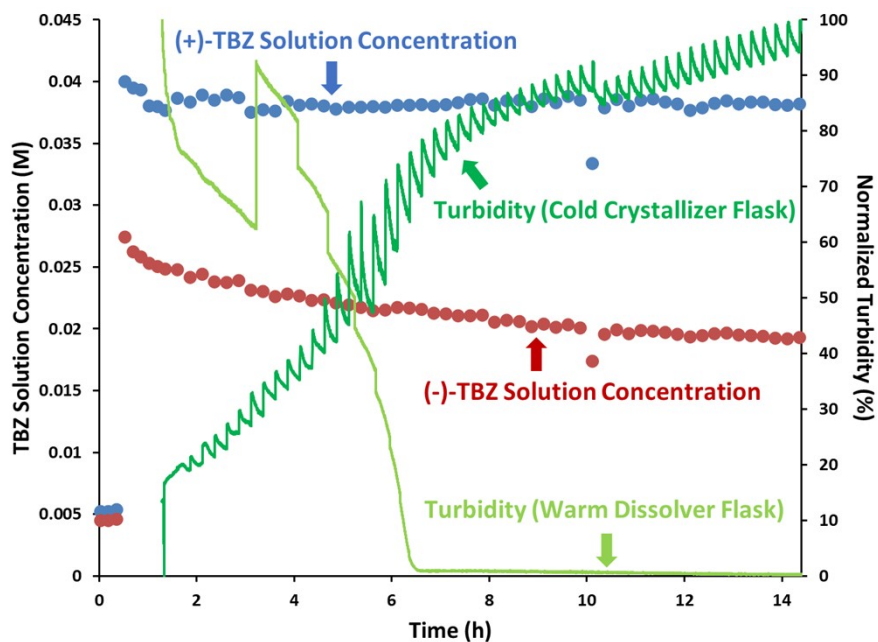


Figure SI 19. CIDT time course data with uncorrected turbidity trend for warm dissolver flask, illustrating controlled solids transfer and crystallization of enantiopure (-)-TBZ•(-)-CSA. Vertical jumps in warm dissolver flask turbidity are due to webcam auto-brightness adjustment.

k. CIDT: Racemization with Dissolver Flask Turbidity Trend

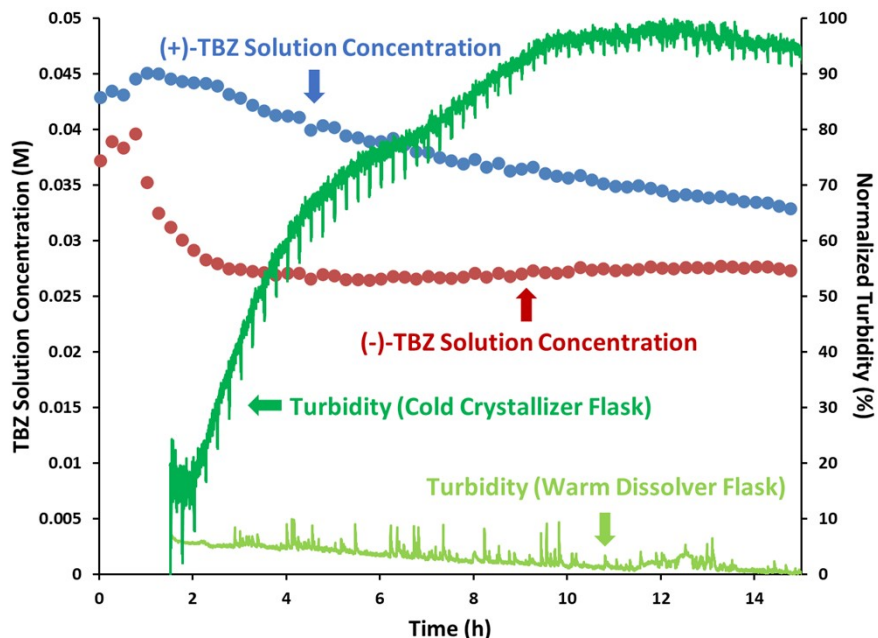


Figure SI 20. CIDT time course data with additional warm dissolver flask turbidity trend (normalized and then divided by 10 to prevent obfuscation of other trends). The warm dissolver flask remained homogeneous throughout the experiment, resulting in perceived amplification of baseline noise.

l. CIDT: Final Experiment Part 1 (Setup)

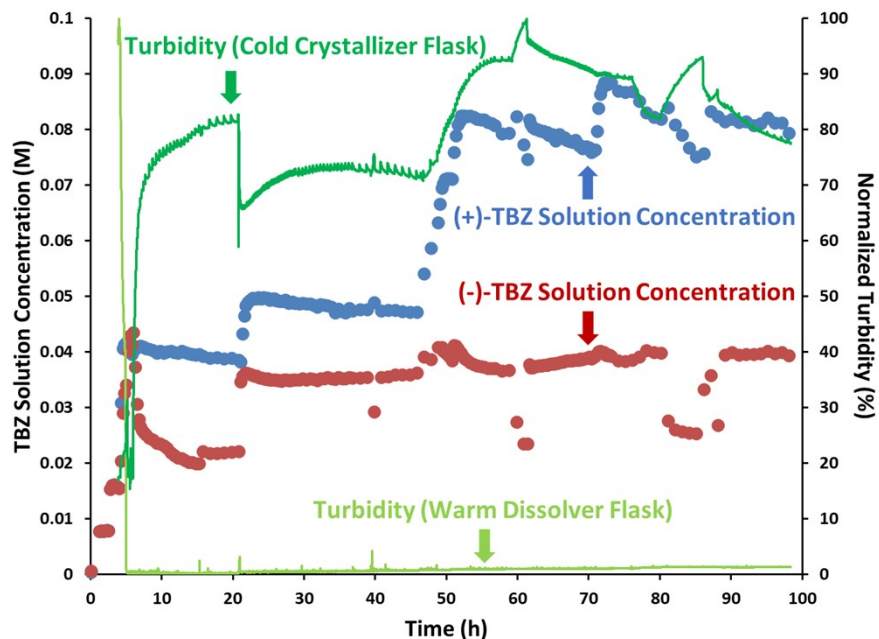


Figure SI 21. CIDT time course data for initial 100 hours of the final CIDT experiment. Dosing of additional racemic TBZ and (-)-CSA to the warm dissolver flask can be seen at 20 h, 45 h and 71 h, with hardware failures occurring at 60 hours (recovered immediately) and 80 hours (recovered after 8 hours).

m. CIDT: Final Experiment Part 2 with Crystallizer Flask Turbidity Trend

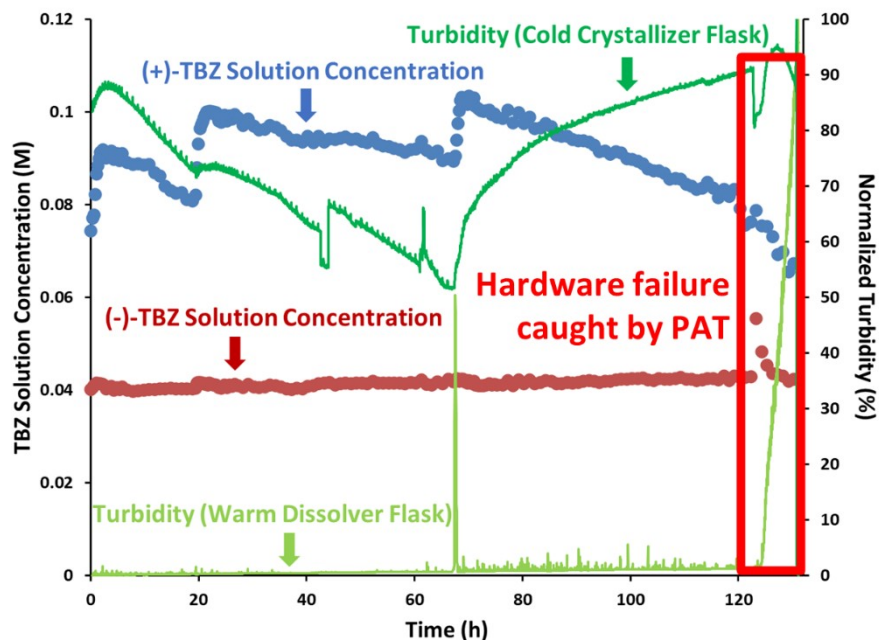


Figure SI 22. CIDT time course data for final CIDT experiment showing subsequent 130 hours of the experiment, with cold crystallizer flask turbidity overlaid. Final hardware failure highlighted is clearly visible from the changes in all PAT trends, and was corrected for immediately after being detected.

8. PXRD Spectra

a. Enantiopure (-)-TBZ•(-)-CSA (3)

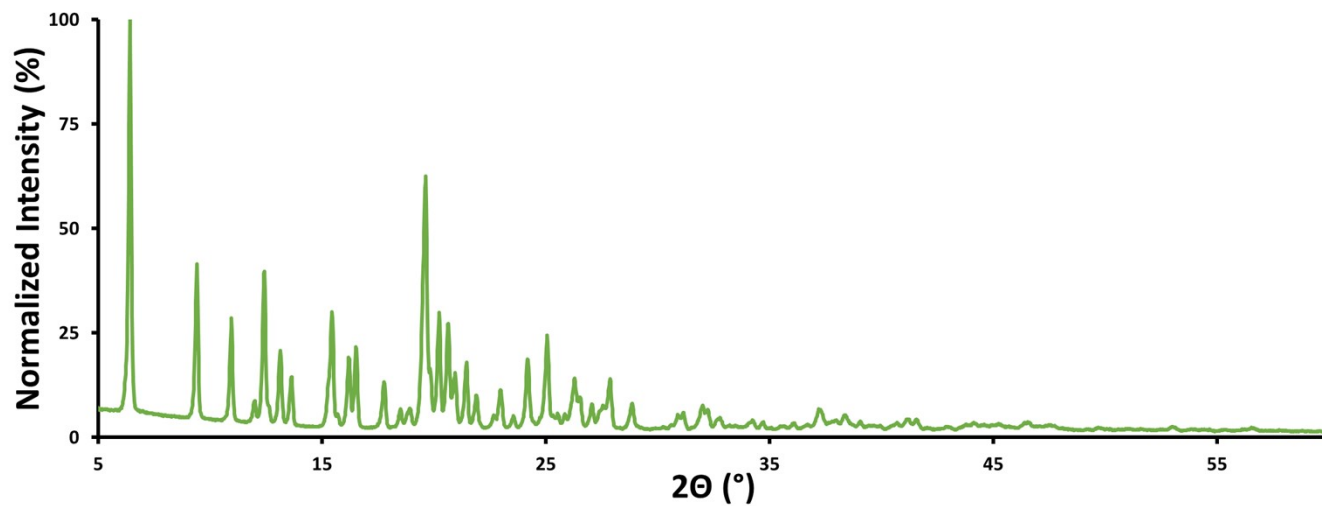


Figure SI 23. PXRD pattern of enantiopure (-)-TBZ•(-)-CSA (3).

b. (-)-TBZ•(-)-CSA, ~0% e.e. (4)

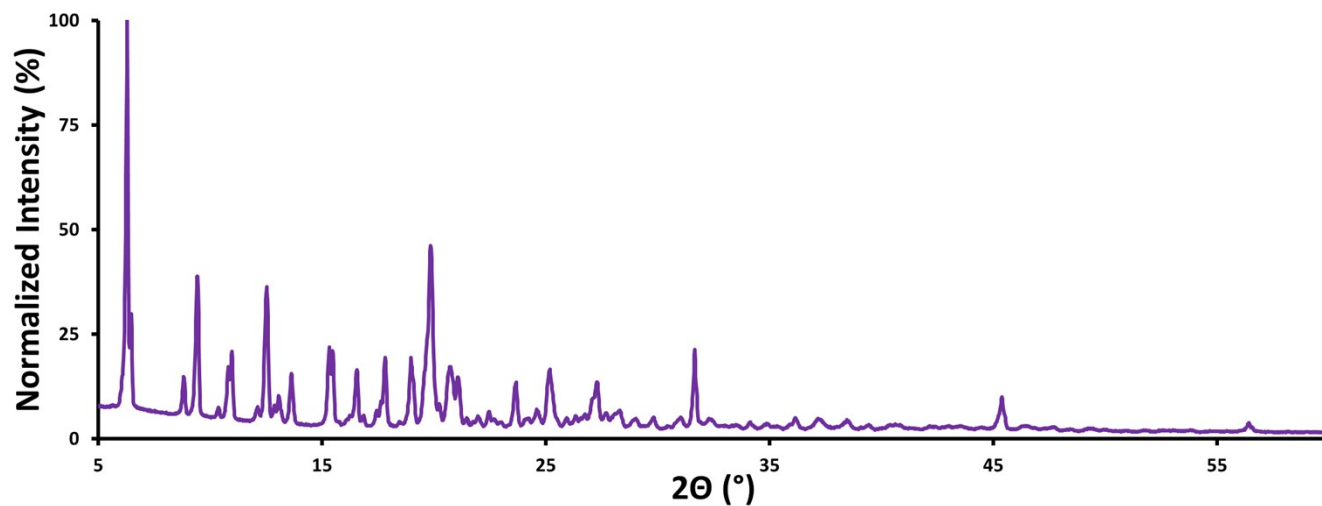


Figure SI 24. PXRD pattern of newly discovered solid phase (+)-TBZ•(-)-TBZ•2 (-)-CSA•2 H₂O (4).

c. Enantiopure vs. Racemic TBZ•(-)-CSA Comparison

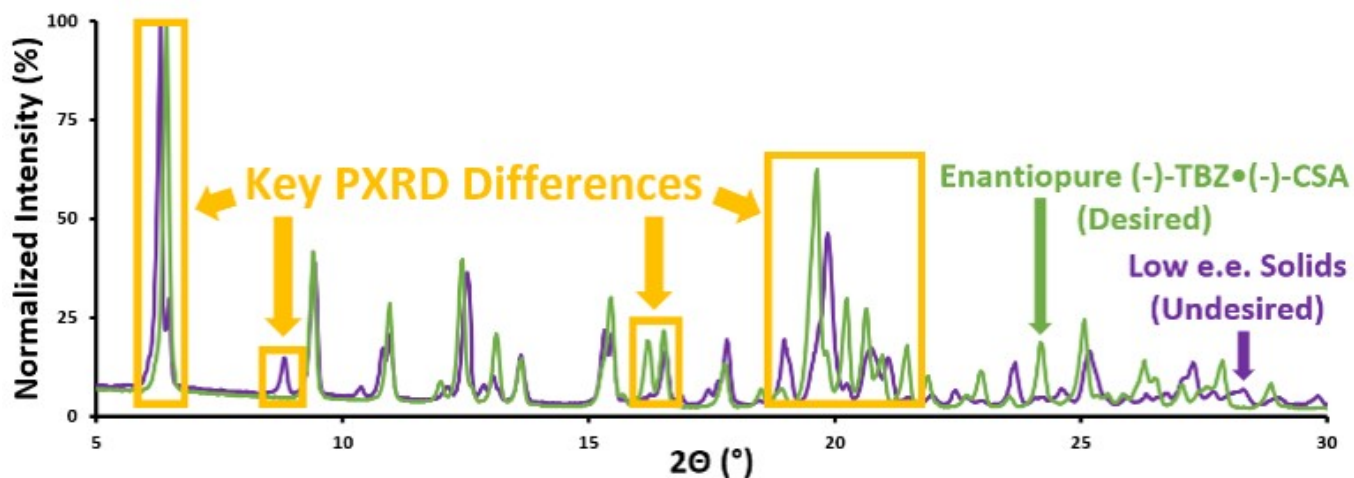


Figure SI 25. Comparison of PXRD patterns for racemic solids with enantiopure (-)-TBZ•(-)-CSA with key differences in PXRD spectra highlighted, showing phases are not the same.

d. (-)-TBZ•(-)-CSA, ~0% e.e. (unknown)

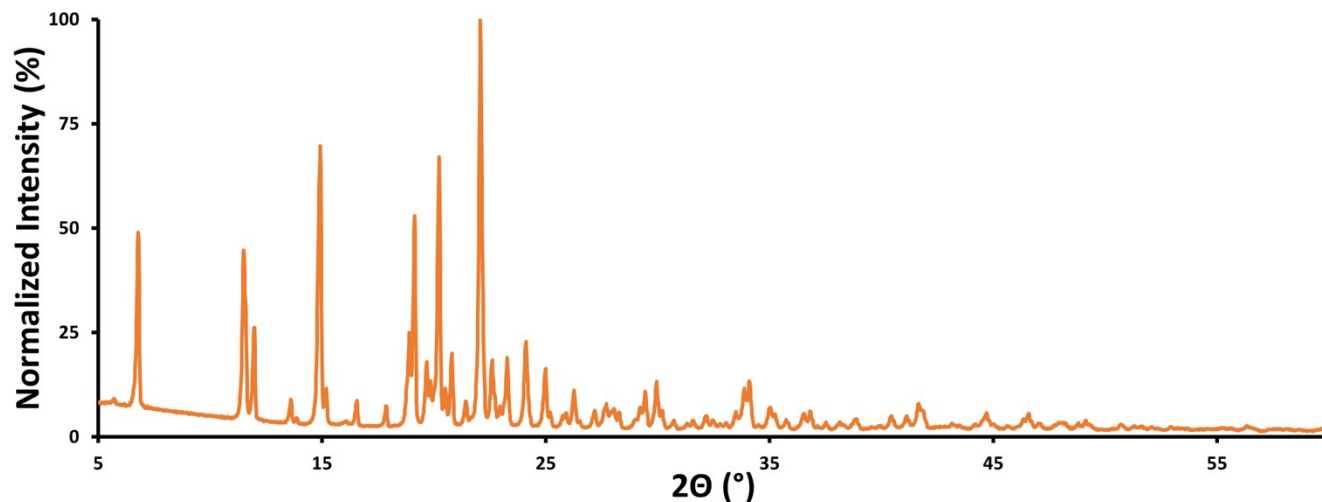


Figure SI 26. PXRD pattern of racemic solids (different from the pattern for 4), suggesting another racemic crystal phase is possible under experimental conditions.

e. Racemic TBZ•(-)-CSA Comparison

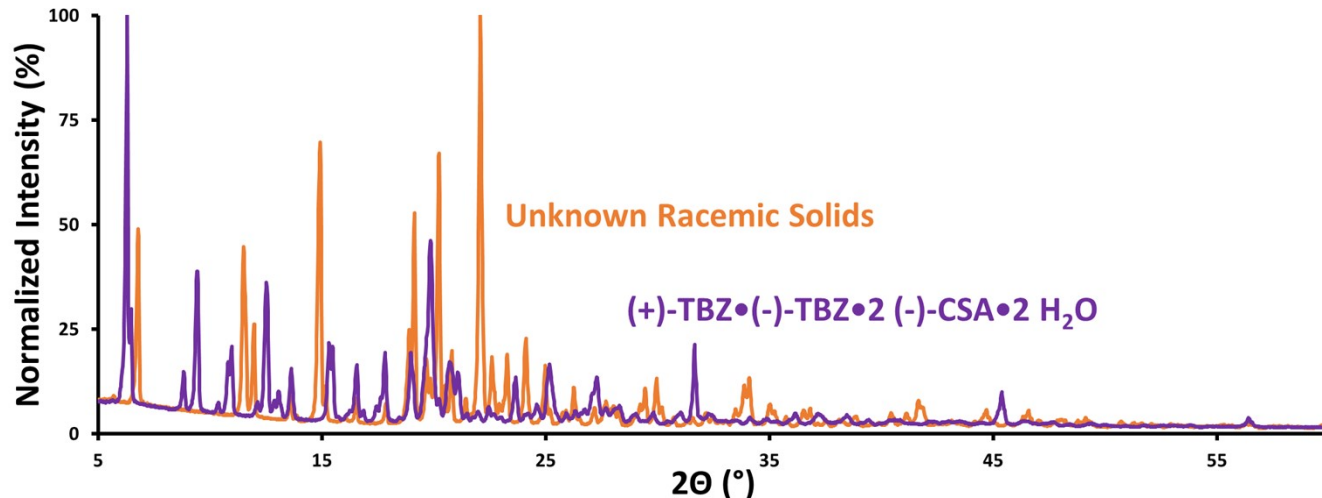


Figure SI 27. Comparison of PXRD patterns for racemic solids, showing phases are not the same.

9. Single Crystal XRD Data - (+)-TBZ•(-)-TBZ•2 (-)-CSA•2 H₂O

A colourless plate-shaped crystal with dimensions $0.21 \times 0.18 \times 0.04 \text{ mm}^3$ was mounted on a MITIGEN holder in oil. Data were collected using a Bruker APEX II area detector diffractometer equipped with an Oxford Cryosystems low-temperature device operating at $T = 90(2) \text{ K}$. Data were measured using ω and ϕ scans of 0.5° per frame for 20 s using MoK_α radiation (TRIUMPH monochromator, sealed X-ray tube, 45 kV, 30 mA). The total number of runs and images was based on the strategy calculation from the program APEX3. The maximum resolution that was achieved was $\Theta = 30.571^\circ$ (0.70 \AA). The unit cell was refined using Bruker's SAINT V8.40B on 9082 reflections, 54% of the observed reflections. The crystal formed and was integrated as a two-component 'split crystal'. Data reduction, scaling and absorption corrections were performed using SAINT V8.40B. The final completeness is 99.20% out to 30.571° in Θ . A multi-scan absorption correction was performed using Bruker's TWINABS-2012/1 was used for absorption correction. Final HKLF 4 output contains 114408 reflections, $R_{int} = 0.0417$ (68615 with $I > 3\text{sig}(I)$, $R_{int} = 0.0341$). The absorption coefficient μ of this material is 0.163 mm^{-1} at this wavelength ($\lambda = 0.71073 \text{ \AA}$) and the minimum and maximum transmissions are 0.908 and 0.994. The structure was solved and the space group $P2_1$ (# 4) determined by the XT structure solution program using Intrinsic Phasing methods and refined by full matrix least squares minimisation on F^2 using version 2018/3 of XL. All non-hydrogen atoms were refined anisotropically. Most hydrogen atom positions were calculated geometrically and refined using the riding model, but some hydrogen atoms were refined freely.

The value of Z' is 2. This means that there are two independent molecules in the asymmetric unit. The Flack parameter was refined to $-0.02(2)$. Determination of absolute structure using Bayesian statistics on Bijvoet differences using the Olex2 results in $0.017(13)$.

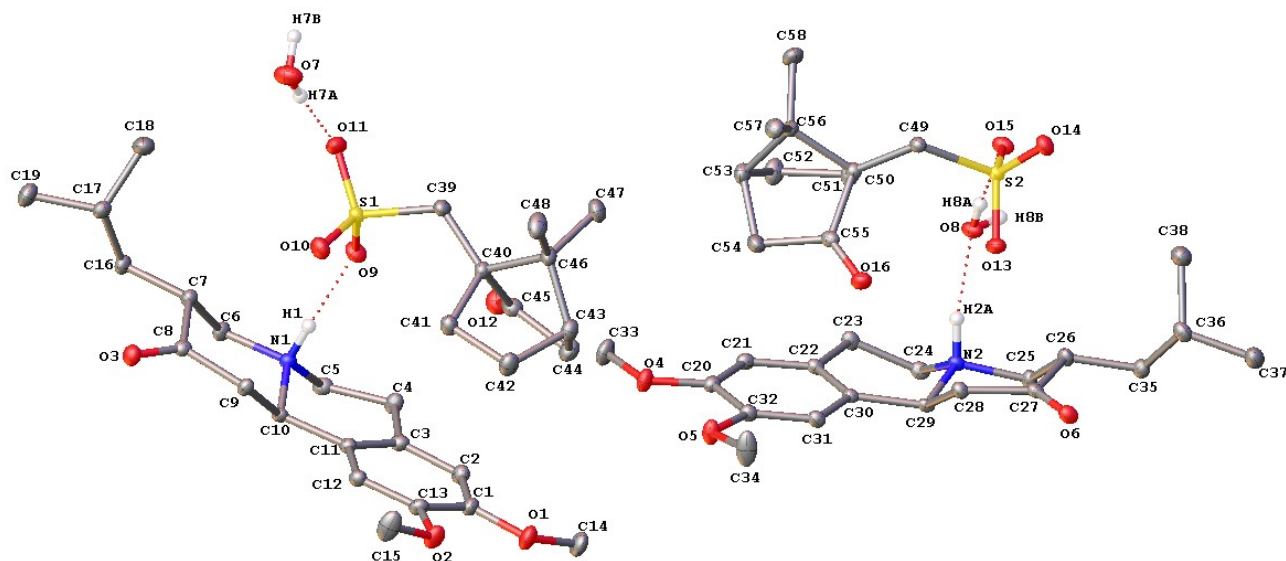


Figure SI 28. Crystal structure of (+)-TBZ•(-)-TBZ•2 (-)-CSA•2 H₂O with atoms labelled. Only key Hydrogen atoms are shown.

Table SI 1. Crystal data and structure refinement for (+)-TBZ•(-)-TBZ•2 (-)-CSA•2 H₂O.

Compound	(+)-TBZ•(-)-TBZ•2 (-)-CSA•2 H ₂ O
Formula	C ₂₉ H ₄₅ NO ₈ S
<i>D</i> _{calc.} / g cm ⁻³	1.310
<i>μ</i> /mm ⁻¹	0.163
Formula Weight	567.72
Colour	colourless
Shape	plate-shaped
Size/mm ³	0.21×0.18×0.04
<i>T</i> /K	90(2)
Crystal System	monoclinic
Flack Parameter	-0.02(2)
Hoofit Parameter	0.017(13)
Space Group	<i>P</i> 2 ₁
<i>a</i> /Å	9.8124(7)
<i>b</i> /Å	10.5313(7)
<i>c</i> /Å	27.852(2)
<i>α</i> [°]	90
<i>β</i> [°]	90.936(2)
<i>γ</i> [°]	90
<i>V</i> /Å ³	2877.8(3)
<i>Z</i>	4
<i>Z</i> '	2
Wavelength/Å	0.71073
Radiation type	MoK α
Θ_{min} [°]	1.462
Θ_{max} [°]	30.571
Measured Refl's.	16775
Indep't Refl's	16775
Refl's I \geq 2 σ (I)	15382
<i>R</i> _{int}	0.042
Parameters	739
Restraints	1
Largest Peak	0.495
Deepest Hole	-0.354
GooF	1.042
<i>wR</i> ₂ (all data)	0.0911
<i>wR</i> ₂	0.0889
<i>R</i> ₁ (all data)	0.0424
<i>R</i> ₁	0.0369

Table SI 2. Fractional Atomic Coordinates ($\times 10^4$) and Equivalent Isotropic Displacement Parameters ($\text{\AA}^2 \times 10^3$) for (+)-**TBZ**•(-)-**TBZ**•2 (-)-**CSA**•2 **H₂O**. U_{eq} is defined as 1/3 of the trace of the orthogonalised U_{ij} .

Atom	x	y	z	U_{eq}
S1	3222.5(5)	4156.5(5)	4538.8(2)	12.79(10)
O9	3469.9(16)	5529.3(16)	4501.8(5)	18.5(3)
O10	1845.4(16)	3859.6(16)	4684.8(5)	19.0(3)
O11	4274.5(16)	3542.1(17)	4834.0(5)	20.3(3)
O12	3676.7(18)	5960.5(17)	3432.3(6)	23.7(3)
C39	3470(2)	3491(2)	3954.5(7)	15.9(4)
C40	2562(2)	3885(2)	3532.0(6)	13.7(4)
C41	995(2)	3981(2)	3616.1(7)	16.7(4)
C42	344(2)	3834(2)	3104.6(7)	20.5(4)
C43	1604(2)	3763(2)	2781.6(7)	17.9(4)
C44	2250(2)	5090(2)	2785.7(7)	20.7(4)
C45	2932(2)	5129(2)	3282.4(7)	16.1(4)
C46	2618(2)	2964(2)	3089.0(6)	15.4(4)
C47	4053(2)	2876(3)	2877.5(7)	22.5(5)
C48	2127(3)	1618(2)	3188.7(8)	23.7(5)
S2	8135.9(5)	2995.8(5)	286.9(2)	11.18(9)
O13	7059.2(15)	3853.4(15)	132.5(5)	16.1(3)
O14	8234.9(15)	1854.5(15)	-11.9(5)	16.3(3)
O15	9455.4(15)	3639.2(15)	341.8(5)	15.8(3)
O16	5092.4(15)	3784.2(16)	946.3(5)	17.4(3)
C49	7732(2)	2380(2)	866.4(6)	11.9(3)
C50	7385(2)	3297.6(19)	1268.3(6)	11.6(4)
C51	8305(2)	4492(2)	1333.4(7)	17.2(4)
C52	8130(3)	4883(2)	1868.2(7)	21.5(4)
C53	7032(2)	3952(2)	2038.2(7)	16.5(4)
C54	5700(2)	4328(2)	1774.1(7)	17.9(4)
C55	5934(2)	3809(2)	1269.1(7)	13.3(4)
C56	7428(2)	2697(2)	1785.3(6)	13.7(4)
C57	6394(2)	1627(2)	1847.2(7)	17.0(4)
C58	8832(2)	2196(2)	1936.6(7)	20.8(5)
O1	-742.1(16)	7444.8(17)	2662.1(5)	20.3(3)
O2	-2366.5(16)	6368.7(17)	3251.8(5)	20.0(3)
O3	-397.2(16)	6037.9(16)	5759.3(5)	17.4(3)
N1	2048.6(17)	7638.0(17)	4758.6(5)	11.5(3)
C1	-343(2)	7503(2)	3135.5(7)	15.6(4)
C2	853(2)	8033(2)	3307.7(7)	15.9(4)
C3	1177(2)	8030(2)	3801.9(6)	13.9(4)
C4	2552(2)	8523(2)	3964.4(7)	16.2(4)
C5	2642(2)	8753(2)	4500.8(7)	14.5(4)
C6	2356(2)	7730(2)	5286.5(6)	14.7(4)

Atom	x	y	z	U_{eq}
C7	1910(2)	6524(2)	5543.9(6)	13.4(4)
C8	403(2)	6298(2)	5446.1(6)	13.2(4)
C9	-33(2)	6375(2)	4921.9(6)	12.7(4)
C10	532.1(19)	7536(2)	4661.4(6)	11.6(3)
C11	261(2)	7510(2)	4121.5(6)	12.3(4)
C12	-958(2)	6961(2)	3947.2(6)	13.3(4)
C13	-1246(2)	6930(2)	3458.1(7)	15.1(4)
C14	77(2)	8123(3)	2328.8(7)	24.0(5)
C15	-3143(3)	5557(3)	3551.7(8)	28.3(6)
C16	2271(2)	6565(2)	6080.0(6)	15.4(4)
C17	2353(2)	5248(2)	6314.7(7)	15.9(4)
C18	3655(3)	4539(3)	6174.0(8)	25.6(5)
C19	2276(3)	5381(3)	6860.1(7)	23.3(5)
O4	4231.5(15)	7579.5(16)	2295.9(5)	17.1(3)
O5	2588.5(15)	6606.5(17)	1672.5(5)	18.3(3)
O6	4946.6(15)	5671.2(15)	-729.6(5)	14.9(3)
N2	7175.1(16)	7728.9(17)	243.8(5)	10.4(3)
C20	4681(2)	7614(2)	1834.7(6)	12.9(4)
C21	5914.2(19)	8081(2)	1686.1(6)	13.3(4)
C22	6283.6(19)	8046(2)	1200.0(6)	11.6(3)
C23	7648(2)	8553(2)	1051.0(7)	14.0(4)
C24	7690(2)	8859(2)	516.7(7)	13.0(4)
C25	7419(2)	7844(2)	-285.1(6)	13.6(4)
C26	7141(2)	6555(2)	-524.9(7)	13.6(4)
C27	5700(2)	6135(2)	-424.6(6)	12.0(3)
C28	5251(2)	6266(2)	89.5(6)	12.5(4)
C29	5685.4(19)	7508(2)	330.5(6)	10.3(3)
C30	5379.3(19)	7532(2)	863.3(6)	11.0(3)
C31	4114.6(19)	7060(2)	1013.0(6)	12.4(4)
C32	3767(2)	7083(2)	1491.2(7)	13.2(4)
C33	5109(2)	8125(3)	2657.1(7)	21.9(5)
C34	1778(3)	5842(3)	1358.3(8)	30.4(6)
C35	7458(2)	6590(2)	-1062.1(7)	15.1(4)
C36	7556(2)	5277(2)	-1296.3(7)	16.9(4)
C37	7576(2)	5420(3)	-1843.5(7)	22.3(5)
C38	8804(2)	4531(3)	-1117.4(8)	23.4(5)
O7	3577.4(19)	1129(2)	5246.9(7)	26.4(4)
O8	9352.8(16)	6233.1(17)	431.0(5)	15.4(3)

Table SI 3. Anisotropic Displacement Parameters ($\times 10^4$) for (+)-**TBZ**•(-)-**TBZ**•**2** (-)-**CSA**•**2** **H₂O**. The anisotropic displacement factor exponent takes the form: $-2\pi^2[h^2a^{*2} \times U_{11} + \dots + 2hka^* \times b^* \times U_{12}]$

Atom	U_{11}	U_{22}	U_{33}	U_{23}	U_{13}	U_{12}
S1	11.9(2)	13.9(3)	12.59(18)	-1.17(16)	0.03(14)	1.36(18)
O9	19.5(8)	13.2(8)	22.8(7)	-3.4(5)	3.3(5)	-0.2(6)
O10	15.9(7)	21.8(9)	19.5(7)	-0.5(6)	5.1(5)	-0.9(6)
O11	19.4(8)	24.5(9)	16.8(7)	-1.1(6)	-4.1(5)	5.8(7)
O12	25.6(9)	20.8(9)	24.6(7)	-0.7(6)	2.4(6)	-5.8(7)
C39	17.6(10)	15.7(11)	14.3(8)	-1.5(7)	0.2(7)	4.3(8)
C40	15.2(9)	13.3(10)	12.7(8)	-0.1(6)	0.3(6)	1.0(7)
C41	14.3(9)	20.7(12)	15.3(8)	-1.3(7)	1.3(6)	-0.9(8)
C42	17.6(10)	27.6(13)	16.1(8)	-0.7(8)	-1.7(7)	-3.8(9)
C43	19.7(10)	20.6(12)	13.3(8)	-0.2(7)	-0.6(7)	-2.8(8)
C44	25.9(11)	19.5(12)	16.9(9)	3.4(7)	-0.4(7)	-1.6(9)
C45	16.5(10)	13.0(11)	18.8(9)	1.0(7)	0.7(7)	-0.7(8)
C46	19.8(9)	13.8(10)	12.8(8)	0.1(7)	2.4(6)	0.7(8)
C47	24.1(11)	25.6(13)	18.0(9)	-3.4(8)	5.3(7)	3.1(10)
C48	36.4(14)	16.7(12)	18.1(9)	-2.6(7)	3.7(8)	-3.2(10)
S2	8.67(19)	11.7(2)	13.22(18)	0.36(15)	1.14(13)	0.91(17)
O13	12.6(7)	18.2(8)	17.6(6)	3.7(5)	0.2(5)	3.5(6)
O14	15.6(7)	16.3(8)	17.0(6)	-4.1(5)	2.7(5)	0.1(6)
O15	10.4(7)	14.5(8)	22.6(7)	1.0(5)	2.2(5)	-0.8(6)
O16	12.7(7)	20.4(9)	19.1(7)	3.4(5)	-0.4(5)	1.4(6)
C49	11.2(8)	11.3(10)	13.2(8)	0.8(6)	1.0(6)	0.4(7)
C50	11.5(8)	10.5(10)	12.7(8)	0.3(6)	0.0(6)	-0.7(7)
C51	18.9(10)	17.5(11)	15.2(8)	-1.5(7)	0.5(7)	-6.2(8)
C52	28.0(12)	18.8(12)	17.7(9)	-3.2(8)	1.2(8)	-7.8(9)
C53	19.5(10)	17.1(11)	12.9(8)	-1.2(7)	1.0(6)	-1.1(8)
C54	19.6(10)	17.1(11)	17.1(9)	-0.3(7)	3.1(7)	5.1(8)
C55	11.9(9)	11.2(10)	16.9(8)	2.6(6)	2.3(6)	-0.5(7)
C56	14.0(9)	14.3(11)	12.9(8)	1.9(6)	-0.3(6)	1.3(7)
C57	18.3(10)	15.4(11)	17.4(9)	3.3(7)	2.7(7)	-1.0(8)
C58	17.0(10)	28.0(13)	17.4(9)	2.8(8)	-4.1(7)	4.2(9)
O1	19.9(8)	28.9(9)	12.0(6)	3.3(6)	-1.1(5)	-4.9(7)
O2	15.1(7)	28.5(10)	16.4(6)	2.8(6)	-3.5(5)	-6.3(7)
O3	16.1(7)	20.9(9)	15.3(6)	2.0(5)	2.1(5)	-2.0(6)
N1	10.1(7)	11.0(9)	13.4(7)	1.0(5)	-0.3(5)	-0.4(6)
C1	16.8(9)	17.7(10)	12.2(8)	1.2(7)	-0.8(6)	1.2(8)
C2	14.8(9)	17.9(10)	15.0(8)	2.8(7)	1.4(6)	-0.7(8)
C3	12.9(8)	12.5(10)	16.4(8)	2.1(7)	-0.3(6)	0.2(8)
C4	13.9(9)	19.9(11)	14.8(8)	2.8(7)	0.1(6)	-5.0(8)
C5	13.7(9)	11.2(10)	18.5(8)	2.1(7)	-0.5(6)	-2.8(7)
C6	15.7(9)	16.0(11)	12.3(8)	-1.1(6)	-2.2(6)	-2.4(8)
C7	13.7(9)	14.4(10)	12.1(8)	0.5(6)	-1.0(6)	-0.1(7)

Atom	U_{11}	U_{22}	U_{33}	U_{23}	U_{13}	U_{12}
C8	14.8(9)	10.7(10)	14.1(8)	0.2(6)	-0.9(6)	0.3(7)
C9	11.2(8)	14.7(10)	12.0(8)	2.1(6)	-0.5(6)	-2.0(7)
C10	8.0(8)	13.4(10)	13.4(7)	1.2(6)	-0.2(6)	0.7(7)
C11	11.5(8)	11.8(10)	13.5(8)	1.4(6)	0.0(6)	0.1(7)
C12	11.1(9)	14.2(10)	14.7(8)	1.7(7)	0.2(6)	-0.2(7)
C13	11.2(9)	16.6(11)	17.2(9)	2.0(7)	-2.1(6)	-0.5(8)
C14	25.1(11)	32.8(14)	14.1(9)	6.6(8)	2.8(7)	-1.8(10)
C15	20.1(11)	42.2(17)	22.5(10)	4.2(10)	-3.3(8)	-17.2(11)
C16	17.0(10)	17.6(11)	11.4(8)	-0.9(7)	-1.8(6)	-0.6(8)
C17	16.4(9)	17.3(11)	14.0(8)	1.0(7)	-2.4(7)	0.6(8)
C18	24.8(12)	29.9(14)	22.1(10)	2.5(9)	-0.9(8)	11.3(10)
C19	27.4(12)	28.1(13)	14.4(9)	2.3(8)	-2.7(8)	-0.5(10)
O4	17.2(7)	23.3(9)	10.7(6)	-0.6(5)	-0.7(5)	-6.2(6)
O5	13.6(7)	27.5(9)	13.9(6)	-2.3(6)	1.6(5)	-8.9(6)
O6	12.0(7)	15.2(8)	17.5(6)	-3.8(5)	-0.4(5)	-0.6(6)
N2	7.6(7)	9.9(9)	13.9(7)	-1.1(5)	-0.2(5)	-0.5(6)
C20	13.9(9)	12.1(10)	12.7(8)	0.4(6)	-1.1(6)	0.2(7)
C21	11.6(8)	13.0(10)	15.3(8)	-1.3(7)	-2.1(6)	-0.3(8)
C22	9.6(8)	10.2(9)	15.1(8)	-1.4(6)	0.3(6)	-0.8(7)
C23	10.4(9)	15.2(10)	16.2(8)	-3.4(7)	0.3(6)	-3.0(8)
C24	11.3(9)	10.2(10)	17.4(8)	-1.6(6)	0.4(6)	-3.0(7)
C25	11.2(8)	17.5(11)	12.2(7)	-0.4(6)	1.5(6)	-1.8(8)
C26	9.6(9)	17.1(10)	14.0(8)	-1.2(7)	1.9(6)	-0.4(7)
C27	10.2(8)	10.3(10)	15.6(8)	-0.7(6)	1.6(6)	1.4(7)
C28	11.4(9)	12.1(10)	14.0(8)	-2.1(6)	1.2(6)	-0.6(7)
C29	6.4(8)	10.3(9)	14.3(7)	-0.2(6)	-0.1(6)	-0.1(7)
C30	9.0(8)	11.0(9)	13.0(7)	-0.1(6)	0.6(6)	1.4(7)
C31	9.8(9)	13.1(10)	14.4(8)	-1.4(6)	-0.1(6)	-1.4(7)
C32	10.4(9)	14.2(10)	15.0(8)	-0.1(7)	-0.2(6)	-1.2(7)
C33	24.1(11)	29.0(13)	12.4(8)	-1.3(8)	-3.9(7)	-8.4(10)
C34	22.1(12)	48.0(18)	21.2(10)	-9.1(10)	4.0(8)	-22.3(12)
C35	13.0(9)	17.5(11)	14.7(8)	0.9(7)	1.9(6)	-1.0(8)
C36	14.1(9)	17.6(11)	19.1(9)	-2.4(7)	3.7(7)	-0.3(8)
C37	20.5(11)	28.5(13)	18.0(9)	-3.0(8)	0.9(7)	4.9(9)
C38	21.9(11)	27.0(13)	21.3(10)	-0.5(8)	2.4(8)	7.0(10)
O7	16.6(9)	24.9(11)	37.7(10)	5.5(7)	0.9(7)	2.9(8)
O8	11.1(7)	13.3(9)	21.8(7)	3.3(5)	2.3(5)	0.7(6)

Table SI 4. Bond Lengths in Å for (+)-TBZ•(-)-TBZ•2 (-)-CSA•2 H₂O.

Atom	Atom	Length/Å
S1	O9	1.4698(17)
S1	O10	1.4516(16)
S1	O11	1.4603(16)
S1	C39	1.792(2)
O12	C45	1.210(3)
C39	C40	1.522(3)
C40	C41	1.562(3)
C40	C45	1.530(3)
C40	C46	1.571(3)
C41	C42	1.560(3)
C42	C43	1.542(3)
C43	C44	1.534(3)
C43	C46	1.550(3)
C44	C45	1.528(3)
C46	C47	1.538(3)
C46	C48	1.524(3)
S2	O13	1.4498(15)
S2	O14	1.4661(16)
S2	O15	1.4672(15)
S2	C49	1.7899(19)
O16	C55	1.211(2)
C49	C50	1.521(3)
C50	C51	1.557(3)
C50	C55	1.522(3)
C50	C56	1.573(3)
C51	C52	1.558(3)
C52	C53	1.537(3)
C53	C54	1.541(3)
C53	C56	1.550(3)
C54	C55	1.530(3)
C56	C57	1.527(3)
C56	C58	1.529(3)
O1	C1	1.371(2)
O1	C14	1.429(3)
O2	C13	1.366(2)
O2	C15	1.424(3)
O3	C8	1.214(2)
N1	C5	1.499(3)
N1	C6	1.499(2)
N1	C10	1.512(2)
C1	C2	1.378(3)
C1	C13	1.408(3)

Atom	Atom	Length/Å
C2	C3	1.408(2)
C3	C4	1.508(3)
C3	C11	1.389(3)
C4	C5	1.514(3)
C6	C7	1.526(3)
C7	C8	1.518(3)
C7	C16	1.530(2)
C8	C9	1.517(2)
C9	C10	1.531(3)
C10	C11	1.523(2)
C11	C12	1.408(3)
C12	C13	1.387(3)
C16	C17	1.535(3)
C17	C18	1.535(3)
C17	C19	1.529(3)
O4	C20	1.365(2)
O4	C33	1.433(2)
O5	C32	1.365(2)
O5	C34	1.422(3)
O6	C27	1.219(2)
N2	C24	1.496(3)
N2	C25	1.501(2)
N2	C29	1.504(2)
C20	C21	1.377(3)
C20	C32	1.415(3)
C21	C22	1.408(2)
C22	C23	1.506(3)
C22	C30	1.390(3)
C23	C24	1.524(3)
C25	C26	1.536(3)
C26	C27	1.513(3)
C26	C35	1.534(3)
C27	C28	1.511(2)
C28	C29	1.527(3)
C29	C30	1.519(2)
C30	C31	1.406(3)
C31	C32	1.380(3)
C35	C36	1.533(3)
C36	C37	1.532(3)
C36	C38	1.531(3)

Table SI 5. Bond Angles in ° for (+)-TBZ•(-)-TBZ•2 (-)-CSA•2 H₂O.

Atom	Atom	Atom	Angle/°
O9	S1	C39	107.23(10)
O10	S1	O9	112.77(10)
O10	S1	O11	113.54(10)
O10	S1	C39	108.09(10)
O11	S1	O9	111.06(10)
O11	S1	C39	103.48(9)
C40	C39	S1	120.59(15)
C39	C40	C41	117.82(16)
C39	C40	C45	116.40(18)
C39	C40	C46	114.26(17)
C41	C40	C46	101.83(16)
C45	C40	C41	104.77(17)
C45	C40	C46	99.21(15)
C42	C41	C40	104.24(15)
C43	C42	C41	102.55(17)
C42	C43	C46	102.55(16)
C44	C43	C42	106.64(19)
C44	C43	C46	103.25(17)
C45	C44	C43	101.89(17)
O12	C45	C40	127.55(19)
O12	C45	C44	125.8(2)
C44	C45	C40	106.53(17)
C43	C46	C40	93.91(16)
C47	C46	C40	112.48(17)
C47	C46	C43	113.86(16)
C48	C46	C40	114.58(16)
C48	C46	C43	113.80(18)
C48	C46	C47	107.92(19)
O13	S2	O14	113.40(9)
O13	S2	O15	112.38(9)
O13	S2	C49	108.78(9)
O14	S2	O15	111.80(9)
O14	S2	C49	103.45(9)
O15	S2	C49	106.35(9)
C50	C49	S2	119.26(14)
C49	C50	C51	117.54(16)
C49	C50	C55	116.50(16)
C49	C50	C56	114.53(16)
C51	C50	C56	102.21(15)
C55	C50	C51	104.75(17)
C55	C50	C56	98.73(15)
C50	C51	C52	104.61(16)

Atom	Atom	Atom	Angle/°
C53	C52	C51	102.39(17)
C52	C53	C54	106.40(18)
C52	C53	C56	102.83(16)
C54	C53	C56	102.65(16)
C55	C54	C53	102.00(16)
O16	C55	C50	128.15(18)
O16	C55	C54	125.39(19)
C50	C55	C54	106.41(16)
C53	C56	C50	94.02(15)
C57	C56	C50	113.10(16)
C57	C56	C53	113.96(17)
C57	C56	C58	108.14(18)
C58	C56	C50	113.68(16)
C58	C56	C53	113.61(17)
C1	O1	C14	116.58(17)
C13	O2	C15	116.56(16)
C5	N1	C6	110.23(15)
C5	N1	C10	111.04(15)
C6	N1	C10	111.20(14)
O1	C1	C2	125.52(18)
O1	C1	C13	114.94(18)
C2	C1	C13	119.52(17)
C1	C2	C3	121.14(18)
C2	C3	C4	118.67(17)
C11	C3	C2	119.27(18)
C11	C3	C4	121.95(16)
C3	C4	C5	112.86(16)
N1	C5	C4	109.31(17)
N1	C6	C7	110.63(16)
C6	C7	C16	111.81(17)
C8	C7	C6	109.43(16)
C8	C7	C16	112.89(16)
O3	C8	C7	123.09(17)
O3	C8	C9	121.87(18)
C9	C8	C7	115.01(16)
C8	C9	C10	113.58(16)
N1	C10	C9	109.59(15)
N1	C10	C11	109.50(15)
C11	C10	C9	113.23(16)
C3	C11	C10	121.40(17)
C3	C11	C12	119.78(17)
C12	C11	C10	118.82(16)
C13	C12	C11	120.45(18)
O2	C13	C1	115.31(17)

Atom	Atom	Atom	Angle [°]
O2	C13	C12	124.94(18)
C12	C13	C1	119.75(19)
C7	C16	C17	113.59(18)
C16	C17	C18	111.63(18)
C19	C17	C16	109.72(18)
C19	C17	C18	110.69(17)
C20	O4	C33	116.77(16)
C32	O5	C34	116.67(16)
C24	N2	C25	112.10(15)
C24	N2	C29	111.28(15)
C25	N2	C29	109.93(14)
O4	C20	C21	126.25(17)
O4	C20	C32	114.52(17)
C21	C20	C32	119.22(17)
C20	C21	C22	121.40(17)
C21	C22	C23	119.97(16)
C30	C22	C21	119.19(17)
C30	C22	C23	120.85(16)
C22	C23	C24	112.48(15)
N2	C24	C23	108.28(16)
N2	C25	C26	108.97(16)
C27	C26	C25	109.76(16)
C27	C26	C35	113.12(16)
C35	C26	C25	111.42(17)
O6	C27	C26	123.14(17)
O6	C27	C28	120.97(18)
C28	C27	C26	115.84(16)
C27	C28	C29	114.31(17)
N2	C29	C28	109.10(15)
N2	C29	C30	111.25(14)
C30	C29	C28	112.68(16)
C22	C30	C29	122.10(17)
C22	C30	C31	119.61(16)
C31	C30	C29	118.24(16)
C32	C31	C30	120.84(17)
O5	C32	C20	115.22(16)
O5	C32	C31	125.05(17)
C31	C32	C20	119.72(18)
C36	C35	C26	114.08(18)
C37	C36	C35	109.63(19)
C38	C36	C35	112.30(18)
C38	C36	C37	110.58(17)

Table SI 6. Torsion Angles in ° for (+)-TBZ•(-)-TBZ•2 (-)-CSA•2 H₂O.

Atom	Atom	Atom	Atom	Angle/°
S1	C39	C40	C41	-44.1(3)
S1	C39	C40	C45	81.7(2)
S1	C39	C40	C46	-163.53(15)
O9	S1	C39	C40	-62.61(19)
O10	S1	C39	C40	59.2(2)
O11	S1	C39	C40	179.93(17)
C39	C40	C41	C42	-157.19(19)
C39	C40	C45	O12	-16.0(3)
C39	C40	C45	C44	160.34(18)
C39	C40	C46	C43	-179.07(17)
C39	C40	C46	C47	-61.2(2)
C39	C40	C46	C48	62.5(2)
C40	C41	C42	C43	-3.7(2)
C41	C40	C45	O12	116.0(2)
C41	C40	C45	C44	-67.62(19)
C41	C40	C46	C43	52.80(18)
C41	C40	C46	C47	170.64(18)
C41	C40	C46	C48	-65.6(2)
C41	C42	C43	C44	-69.8(2)
C41	C42	C43	C46	38.3(2)
C42	C43	C44	C45	74.9(2)
C42	C43	C46	C40	-56.22(19)
C42	C43	C46	C47	-172.91(19)
C42	C43	C46	C48	62.8(2)
C43	C44	C45	O12	173.1(2)
C43	C44	C45	C40	-3.4(2)
C44	C43	C46	C40	54.50(17)
C44	C43	C46	C47	-62.2(2)
C44	C43	C46	C48	173.56(17)
C45	C40	C41	C42	71.6(2)
C45	C40	C46	C43	-54.53(17)
C45	C40	C46	C47	63.3(2)
C45	C40	C46	C48	-172.95(19)
C46	C40	C41	C42	-31.4(2)
C46	C40	C45	O12	-139.1(2)
C46	C40	C45	C44	37.3(2)
C46	C43	C44	C45	-32.8(2)
S2	C49	C50	C51	-44.7(2)
S2	C49	C50	C55	80.9(2)
S2	C49	C50	C56	-164.68(14)
O13	S2	C49	C50	-52.27(17)
O14	S2	C49	C50	-173.10(15)

Atom	Atom	Atom	Atom	Angle/°
O15	S2	C49	C50	68.99(17)
C49	C50	C51	C52	-156.09(18)
C49	C50	C55	O16	-15.7(3)
C49	C50	C55	C54	161.90(17)
C49	C50	C56	C53	179.70(16)
C49	C50	C56	C57	-62.1(2)
C49	C50	C56	C58	61.7(2)
C50	C51	C52	C53	-5.0(2)
C51	C50	C55	O16	116.1(2)
C51	C50	C55	C54	-66.37(19)
C51	C50	C56	C53	51.47(17)
C51	C50	C56	C57	169.66(17)
C51	C50	C56	C58	-66.5(2)
C51	C52	C53	C54	-68.5(2)
C51	C52	C53	C56	39.0(2)
C52	C53	C54	C55	75.8(2)
C52	C53	C56	C50	-55.86(17)
C52	C53	C56	C57	-173.35(16)
C52	C53	C56	C58	62.2(2)
C53	C54	C55	O16	172.8(2)
C53	C54	C55	C50	-4.9(2)
C54	C53	C56	C50	54.49(17)
C54	C53	C56	C57	-63.0(2)
C54	C53	C56	C58	172.53(17)
C55	C50	C51	C52	72.77(19)
C55	C50	C56	C53	-55.80(17)
C55	C50	C56	C57	62.4(2)
C55	C50	C56	C58	-173.78(18)
C56	C50	C51	C52	-29.8(2)
C56	C50	C55	O16	-138.8(2)
C56	C50	C55	C54	38.8(2)
C56	C53	C54	C55	-31.9(2)
O1	C1	C2	C3	-179.2(2)
O1	C1	C13	O2	1.8(3)
O1	C1	C13	C12	-178.5(2)
O3	C8	C9	C10	135.3(2)
N1	C6	C7	C8	-56.8(2)
N1	C6	C7	C16	177.35(16)
N1	C10	C11	C3	-24.3(3)
N1	C10	C11	C12	156.62(18)
C1	C2	C3	C4	174.9(2)
C1	C2	C3	C11	-1.5(3)
C2	C1	C13	O2	-176.5(2)
C2	C1	C13	C12	3.2(3)

Atom	Atom	Atom	Atom	Angle [°]
C2	C3	C4	C5	166.6(2)
C2	C3	C11	C10	-177.2(2)
C2	C3	C11	C12	1.9(3)
C3	C4	C5	N1	45.7(2)
C3	C11	C12	C13	0.3(3)
C4	C3	C11	C10	6.6(3)
C4	C3	C11	C12	-174.4(2)
C5	N1	C6	C7	-173.08(16)
C5	N1	C10	C9	178.90(15)
C5	N1	C10	C11	54.1(2)
C6	N1	C5	C4	169.58(17)
C6	N1	C10	C9	-58.0(2)
C6	N1	C10	C11	177.27(17)
C6	C7	C8	O3	-132.8(2)
C6	C7	C8	C9	49.2(2)
C6	C7	C16	C17	-158.18(18)
C7	C8	C9	C10	-46.7(2)
C7	C16	C17	C18	74.3(2)
C7	C16	C17	C19	-162.58(18)
C8	C7	C16	C17	77.9(2)
C8	C9	C10	N1	49.2(2)
C8	C9	C10	C11	171.80(17)
C9	C10	C11	C3	-146.9(2)
C9	C10	C11	C12	34.0(3)
C10	N1	C5	C4	-66.7(2)
C10	N1	C6	C7	63.3(2)
C10	C11	C12	C13	179.4(2)
C11	C3	C4	C5	-17.2(3)
C11	C12	C13	O2	176.8(2)
C11	C12	C13	C1	-2.8(3)
C13	C1	C2	C3	-1.0(3)
C14	O1	C1	C2	-7.8(3)
C14	O1	C1	C13	174.0(2)
C15	O2	C13	C1	167.1(2)
C15	O2	C13	C12	-12.6(3)
C16	C7	C8	O3	-7.6(3)
C16	C7	C8	C9	174.39(18)
O4	C20	C21	C22	178.8(2)
O4	C20	C32	O5	-0.7(3)
O4	C20	C32	C31	-179.74(19)
O6	C27	C28	C29	-140.0(2)
N2	C25	C26	C27	57.4(2)
N2	C25	C26	C35	-176.49(16)
N2	C29	C30	C22	16.7(3)

Atom	Atom	Atom	Atom	Angle [°]
N2	C29	C30	C31	-165.72(17)
C20	C21	C22	C23	-179.3(2)
C20	C21	C22	C30	0.3(3)
C21	C20	C32	O5	178.00(19)
C21	C20	C32	C31	-1.0(3)
C21	C22	C23	C24	-160.39(19)
C21	C22	C30	C29	177.62(19)
C21	C22	C30	C31	0.1(3)
C22	C23	C24	N2	-50.6(2)
C22	C30	C31	C32	-0.9(3)
C23	C22	C30	C29	-2.8(3)
C23	C22	C30	C31	179.71(19)
C24	N2	C25	C26	168.45(16)
C24	N2	C29	C28	-173.84(15)
C24	N2	C29	C30	-48.9(2)
C25	N2	C24	C23	-169.38(15)
C25	N2	C29	C28	61.4(2)
C25	N2	C29	C30	-173.71(16)
C25	C26	C27	O6	136.7(2)
C25	C26	C27	C28	-46.0(2)
C25	C26	C35	C36	165.28(17)
C26	C27	C28	C29	42.6(2)
C26	C35	C36	C37	168.26(17)
C26	C35	C36	C38	-68.4(2)
C27	C26	C35	C36	-70.5(2)
C27	C28	C29	N2	-48.4(2)
C27	C28	C29	C30	-172.51(16)
C28	C29	C30	C22	139.6(2)
C28	C29	C30	C31	-42.8(2)
C29	N2	C24	C23	67.0(2)
C29	N2	C25	C26	-67.2(2)
C29	C30	C31	C32	-178.56(19)
C30	C22	C23	C24	20.0(3)
C30	C31	C32	O5	-177.5(2)
C30	C31	C32	C20	1.4(3)
C32	C20	C21	C22	0.2(3)
C33	O4	C20	C21	2.4(3)
C33	O4	C20	C32	-178.96(19)
C34	O5	C32	C20	-167.6(2)
C34	O5	C32	C31	11.3(3)
C35	C26	C27	O6	11.6(3)
C35	C26	C27	C28	-171.13(18)

Table SI 7. Hydrogen Fractional Atomic Coordinates ($\times 10^4$) and Equivalent Isotropic Displacement Parameters ($\text{\AA}^2 \times 10^3$) for (+)-**TBZ**•(-)-**TBZ**•**2** (-)-**CSA**•**2** **H₂O**. U_{eq} is defined as 1/3 of the trace of the orthogonalised U_{ij} .

Atom	x	y	z	U_{eq}
H39A	4422.17	3672.9	3864.88	19
H39B	3391.95	2557.3	3986.32	19
H41A	685.61	3295.69	3831.84	20
H41B	756.75	4811.67	3758.25	20
H42A	-208.63	3049.84	3079.73	25
H42B	-234.5	4573.89	3020.68	25
H43	1415.22	3413.56	2453.44	21
H44A	2925.64	5181.94	2528	25
H44B	1549.64	5762.37	2750.1	25
H47A	4398.33	3732.95	2815.58	34
H47B	4010.86	2396.98	2576	34
H47C	4663.79	2442.9	3106.01	34
H48A	2831.63	1156.91	3371.04	35
H48B	1944.77	1180.82	2883.78	35
H48C	1289.84	1651.75	3375.21	35
H49A	6949.24	1794.93	823.99	14
H49B	8516.55	1861.76	978.23	14
H51A	8004.36	5182.73	1115.34	21
H51B	9268.98	4285.81	1267.58	21
H52A	8991.35	4776	2054.02	26
H52B	7819.91	5774.08	1895.53	26
H53	6955.51	3885.36	2394.89	20
H54A	4898.04	3926.68	1922.71	22
H54B	5575.2	5260.94	1769.99	22
H57A	5489.76	1920.62	1741.91	26
H57B	6366.88	1380.02	2186.16	26
H57C	6662.53	894.95	1653.39	26
H58A	8987.29	1369.72	1784.87	31
H58B	8874.91	2100.01	2286.55	31
H58C	9534.79	2795.66	1835.45	31
H2	1468.4	8406.73	3089.07	19
H4A	2741.9	9328.45	3794.73	19
H4B	3261.59	7902.89	3874.2	19
H5A	3606.46	8869.64	4601.36	17
H5B	2134.8	9533.51	4582.91	17
H6A	1873.3	8470.35	5421.78	18
H6B	3346.6	7859.17	5338.74	18
H7	2419.36	5797.85	5401.03	16
H9A	-1041.19	6396.69	4901.22	15
H9B	274.25	5597.49	4755.53	15

Atom	x	y	z	U_{eq}
H10	86.01	8310.29	4794.9	14
H12	-1587.38	6608.18	4165.95	16
H14A	-329.89	8054.57	2006.21	36
H14B	997.34	7761.64	2328.97	36
H14C	125.7	9019.2	2422.79	36
H15A	-3850.97	5132.35	3358.53	42
H15B	-3569.5	6062.16	3803.67	42
H15C	-2541.61	4919.01	3699.09	42
H16A	1576.26	7075.76	6246.8	18
H16B	3159.93	6997.47	6123.89	18
H17	1550.37	4739.58	6200.72	19
H18A	3663.06	4425.63	5824.89	38
H18B	3676.8	3707	6331.21	38
H18C	4454.43	5033.51	6276.21	38
H19A	3010.16	5938.46	6975.82	35
H19B	2373.76	4542.79	7009.54	35
H19C	1393.2	5747	6944.66	35
H21	6529.28	8435.3	1916.52	16
H23A	8360.55	7917	1129.03	17
H23B	7856.79	9332.15	1237.06	17
H24A	7111.57	9607.7	444.29	16
H24B	8635.15	9056.34	422.72	16
H25A	8372.86	8105.91	-339.98	16
H25B	6807.29	8497.9	-426.06	16
H26	7771.11	5921.93	-371.44	16
H28A	5630.74	5548.56	278.27	15
H28B	4245.24	6201.71	97.24	15
H29	5163.18	8213.83	173.3	12
H31	3491.4	6720.19	782.08	15
H33A	5236.29	9030.34	2590.07	33
H33B	5993.94	7694.31	2655.4	33
H33C	4695.53	8023.13	2972.73	33
H34A	1384.97	6373.81	1102.58	46
H34B	1043.59	5445.19	1539.25	46
H34C	2347.76	5181.06	1216.42	46
H35A	6737.86	7083.97	-1230.8	18
H35B	8332.52	7042.11	-1105.6	18
H36	6722.84	4784.17	-1211.37	20
H37A	6761.82	5883.92	-1952.28	34
H37B	7585.59	4577.85	-1992.93	34
H37C	8392.81	5890.9	-1935.4	34
H38A	9632.85	5014.27	-1184.92	35
H38B	8838.15	3710.01	-1282.08	35
H38C	8739.92	4392.91	-770.52	35

Atom	x	y	z	U_{eq}
H1	2430(30)	6890(30)	4676(10)	23(7)
H8A	9420(30)	5500(40)	416(11)	28(9)
H2A	7700(30)	7030(30)	332(10)	21(7)
H8B	10130(40)	6510(40)	291(12)	39(9)
H7A	3780(40)	1850(40)	5146(12)	38(9)
H7B	4350(40)	840(40)	5300(11)	35(9)

Table SI 8. Hydrogen Bond information for (+)-TBZ•(-)-TBZ•2 (-)-CSA•2 H₂O.

D	H	A	d(D-H)/Å	d(H-A)/Å	d(D-A)/Å	D-H-A/deg
N1	H1	O9	0.91(3)	1.83(3)	2.724(2)	170(3)
O8	H8A	O15	0.78(4)	1.97(4)	2.745(2)	175(3)
N2	H2A	O8	0.93(3)	1.85(3)	2.699(2)	152(3)
O8	H8B	O14 ¹	0.90(4)	1.84(4)	2.736(2)	173(3)
O7	H7A	O11	0.83(4)	2.05(4)	2.876(3)	174(3)
O7	H7B	O9 ²	0.83(4)	2.22(4)	3.036(2)	166(4)

¹2-x,1/2+y,-z; ²1-x,-1/2+y,1-z

Table SI 9. Absolute configuration assignments for (+)-TBZ•(-)-TBZ•2 (-)-CSA•2 H₂O.

Atom	Config.	Atom	Config.
N1	S	N2	S
C7	R	C40	R
C10	R	C43	S
C26	R	C50	R
C29	S	C53	S

10. References

1. Y. Sato, J. Liu, A. J. Kukor, J. C. Culhane, J. L. Tucker, D. J. Kucera, B. M. Cochran, J. E. Hein, *J. Org. Chem.* **2021**, *86*, 14069–14078.
2. A. J. Kukor, M. A. Guy, J. M. Hawkins, J. E. Hein, *React. Chem. Eng.* **2021**, *6*, 2042–2049.
3. P. Shiri, V. Lai, T. Zepel, D. Griffin, J. Reifman, S. Clark, S. Grunert, L. P. E. Yunker, S. Steiner, H. Situ, P. L. Prieto, J. E. Hein, *iScience* **2021**, *24*, 3.
4. Z. Yao, X. Wei, X. Wu, J. L. Katz, T. Kopajtic, N. H. Greig, H. Sun, *Eur. J. Med. Chem.* **2011**, *46* (5), 1841–1848.